Politecnico Di Torino`

College of Land, Environment and Infrastructure Engineering

Master of Petroleum Engineering

Parallel matlab code for seismic tomography data inversion

A master thesis submitted as partial fulfillment for the degree of Master of Science degree in Petroleum Engineering

Student Name: Mohammed E. Adam

Supervisor Name: Professor. GODIO ALBERTO

Dec.2018

Abstract

The objective of the thesis is to verify the effectiveness of staggered grid mesh applied to two known inversion methods in resolution enhancement. The staggered grid is an approach to enhance resolution and smoothness by averaging several coarse grid inversion solutions by shifting an original grid in both directions in case of 2D inversion without risk of undetermination associated with a fine grid. In this thesis we have taken an overview about the traveltime seismic tomography, with a focus on crosshole tomography and the use of staggered grid for inversion enhancement. The practical work was to improve some properties of an already developed matlab code (SGRAT), which is stand for Staggered Grid Random Tomography invented by Godio Alberto, and Luigi Sambuelli 2011; besides recovering some running errors and an application to synthetic and real field datasets. Some minor running errors have been recovered in forward modelling, conjugated gradient inversion tools regarding the velocity modelling and ray tracing and displaying the results. Plots for spatial coverage (total length per pixel) and ray density (total number of rays per pixel) have been introduced to the simultenious iterative reconustruction technique SIRT. Two data sets have been tested on SIRT inversion first then SIRT staggered random inversion and regular SIRT staggered inversion; results show some kind of resolution improvement measured by root mean square of data errors and velocity map image smoothness. Some open issues recommended to be investigated are the reliability of the conjugated gradient inversion method, effect of parallel computing on reducing computation time.

Table of Contents

List of Tables

List of Figures

1.Chapter One: Introduction

1.Chapter One: Introduction

1.1. Seismic tomography:

Historical definition of the term tomography roots from a Greek origin "**tomos**" meaning "slice" (C. Thurber, and J. Ritsema, 2007) . Basically, seismic tomography term may take practical meaning; an imaging tool that uses seismic waves generated by earthquakes or explosions to create computer-generated images of Earth's interior (C. Thurber, and J. Ritsema, 2007). Where Seismic tomography is one of the important techniques to investigate the distribution of physical properties that affect seismic-wave propagation such as velocity and density, tomography models often play a critical role in the analysis of the subsurface physical properties lithology, temperature, fracturing, fluid content, etc.

Seismic tomography can be classified into two main categories; travel time tomography and amplitude tomography. With regard to the first category seismic travel time tomography is defined as Earth's velocity model reconstruction based on Initial guess of velocity as one of characteristic model input and by use of seismic waves travel time deviations from this reference velocity model (M. Aravinitis, B.D. Al-Nazi, 2009)

Physical classification in lieu with the nature of the seismic waves, travel time tomography can be divided into: straight (mostly in crosshole), signal refraction, signal reflection, and signal diffraction. Referring to the source, whether it is a natural earthquake or artificial seismic wave source, classified up tomography into passive and active tomography, respectively (M. Aravinitis, B.D. Al-Nazi, 2009).

1.2. Problem Statement:

The typical outcome of seismic tomography inversion is a 2D image or 3D volume representing velocity distribution or any other property. The quality of the image depends on the quality of the observations, coverage and the accuracy of the modeling tool (Tape, 2009). The Measurement of the quality of the image and the solution can be done by several tools like coverage, stability, robustness, solution uncertainity and image resolution. The resolution of this seismic tomography image is very important in geological interpretation of the model since it is supposed to study velocity distribution, anisotropy structures and attenuation (Zhao, 2015).

Because the model developed on by dividing up the certain region to be investigated into small parts parameter specified value in case of forward problem or to be estimated in case of inverse problem, in fact that increasing number of parts (cells) or pixels enhances information's by enforcing details gotten from it since the parameter in each cell is assumed to be constant, the increment of the pixels, will lead to consider more pixels in the computation of travel paths for each receiver (Imhof et al, 2010) and so lead to some computation problems.

The discretization of the inverse model domain plays a critical role to a successful model, and the reliability of the result is affected by the chosen mesh. Of course, a fine cells grid may enhance the detail of a model but reduces the model resolution (Arato et al, 2014). The optimal solution which we are looking for is to invert on a grid that provides both high resolution and detail without affecting model construction and resolution. Our current resolution is cumbersome, thus, in this research work, model resolution represents thesis problem.

1.3. **Methodology (the proposed solution):**

The primary objective of this thesis is to develop an old matlab code implementing inversion process using both regular and irregular grid with regular and random parameterization utilizing two well known inversion algorithms: simultenuous iterative reconstruction technique (SIRT); and conjugated gradient (CG). Furthermore the code has the capability to apply a novel technique known as staggered grid in purpose of study the reliability and the resolution of the two methods of inversion. The second objective is to test the reliability of the data inversion algorithm and resolution enhancement after the application of staggered grid inversion. The test will take place in two datasets, syntheic model generated by the forward modeling tool of the code and field data collected in context of another experiment.

The staggered grid method has been used in previous studies to enhance resolution and smoothness of inversion solutions in a variety of fields, optics, resistivity and even seismic tomography. With grid staggering, the image quality will be enhanced because the final result is obtained by averaging the model parameter of several inversions carried out on many coarse grid models. Moreover, the reduction in the number of model cells contributes to limiting the under-determination of the problem. Furthermore, the possibility to average the various solutions and to check the dispersion of the model parameter distribution which in our case velocity or slowness in each cell can be useful in reducing the possible non-uniqueness of the

solutions without constraining the model with a priori information (Arato et al, 2014). Therefore a larger amount of information from the final model with many possibilities can be obtained without the risk of biassing the estimated image from a single model.

1.4. Thesis strucure:

The first chapter is an introduction to seismic tomography as a concept with focus in the quality of the outcome image and how to enhance the resolution and the convergence to the observed data with avoidance of infecting the mathematical manipulation that lead to undetermination of the problem.The statement of the problem under research and the proposed procedures and methodology to achieve the research objectives, and breif description of thesis structure.

The second chapter will discuss the seismic travel time inversion and explanation of inversion procedure in a detailed manner, by passing through common inversion algorithms like back projection and Gradient methods and their invariants.

The third chapter will go in detail with a special spatial configuration of seismic tomography well known as cross-hole seismic inversion and its application in engineering fields associated with a detailed discussion of its resolution analysis.

The fourth chapter is an attempt to apply staggered grid inversion in a seismic cross-hole tomography to increase its resolution. It will start with introduction to SGRAT software for staggered grid seismic data inversion with breif summary of some development and improvement carried out for the original version of the software. Furthermore, an appliction on synthetic data and real field data will be analyzed to verify the effectivness of the method.

2.Chapter Two: Seismic Traveltime Tomography

2. Chapter Two: Seismic Travel time Tomography

2.1. Introduction

The goal of seismic travel-time tomography is to find a velocity model for a subsurface volume or cross section consistent with measured traveltimes along ray paths that pass through the volume (R. L. Nowack, and C. Li, 2009). Today, a lot of methods exist for determining Earth structure from seismic traveltimes.

In general, a study of seismic tomography according to (Zhao, 2015) includes the following steps:

1- Model parameterization by assigning a reference or primary value to the model.
2- Forward modeling to produce synthetic data to be correlated to the observations
3- Inversion operation by the aim to estimate model parameters by solving the large system of observation equations.
4- Resolution and error evaluation, by checking uncertainty and sensitivity of the obtained tomographic solution.

2.2. Model parameterization:

Model parameterization means to set an initial model parameter distribution in a way that care and represents the earth heterogenities and anistropies. In fact Earth has structural and lithological heterogenities on different spatial scales, including complications such as discontinuities, faults, layering, intrusions, inclusions, zones of excess temperature and random geological heterogeneities. This heterogenity has been represented with different ways of parameterization whether in 2D or 3D tomography schemes. It is difficult to represents the heterogenities on a single scheme according to (C. Thurber, and J. Ritsema, 2007). This parameterization can be in regular or irregular.

Generally the parameterization can be divided into two forms of representation (Imhof et al, 2010):

a) Parametric based: depends on asigning a constant host velocity, and constant inclusion velocity, with spatial parameters to constrain dimensions and location. This will lead to an over-determined system of equations that can be solved with variational or least

squares inversion algorithms. This approach has the advantage of simplicity but is clearly lacking the ability to represent heterogeneous structure faithfully, even structures as simple as slight gradients in velocity or oblique discontinuities (C. Thurber, and J. Ritsema, 2007).

b) Pixel based: The medium is divided in a number of uniform pixels; each of them is an unknown with a particular velocity or slowness value to be estimated by the inversion process and represented in a colour pattern as a tomogram. It is clear that the smaller the pixels, the better the image resolution obtained, but the cost of pixel increment is an under-determined system of equations.

A mix of both approaches can be conducted in order to avoid under parametrization and under determination. Reference to the common non uniform geometry of sources and recievers, missing data, and bended ray path, mostly a seismic tomography problem is uneven.and so some nodes or cells might not be sampled, while others may be sampled repeatedly. The pure pixel parametrization approach faces some difficulties to minimize misfit of uneven sampling inverse model; and thus affect the stability of the solution (C. Thurber, and J. Ritsema, 2007).

With increasing seismic datasets scale, the digree of heterogenity will increase of course, giving inequal resolvibility. For a better parameterisation to these resolution variations; a kind of irregular mesh has been introduced; some potential benefits for irregular parameterization are increasing computational efficiency by use fewer unknowns, and un improvement of stability of the inverse problem, moreover a better interpretation can be obtained because of structural compatibility with meshing, examples of these meshes are Delaunay tetrahedra or Voronoi polyhedra, that offer high levels of adaptability (C. Thurber, and J. Ritsema, 2007).

2.3. Forward modeling and ray tracing:

The forward problem in seismic tomography is a calculation of synthetic model data that best fitting the observations, given a set of values for the model parameters. When we are coming to traveltime tomography, the aim is to compute traveltimes based of source reciever geometry for a given velocity model. This action can be done using some form of ray tracing or wavefront tracking. Generally there are three approaches based on ray transmission used for large scales of seismic tomography which investigates deep crust and mantle: Shooting methods based on

Snell's law of refraction, bending methods based on Fermat's principle, Full wave equation methods based on Huygen's principle (Berryman, 1991).

But in our case of cross-hole tomography we adopted a rectlinear raytracing approach considering a semi homoginuous or very small variation of velocity distribution in such a way the refraction will be negligible.

The forward problem is to produce a traveltime vector according to the formula (2.1):

$$d = G(m) \qquad (2.1)$$

Where:

d observations vector, **G** is a forward operator, and **m** is a given model parameter. This formula can be expressed in terms of traveltime and the forward operator to be considered is the ray path as in formula (2).

$$t = \int \frac{1}{v(x)} dx \qquad (2.2)$$

t represinting travel time, the forward operator is the reciprocal of the velocity v(x), which is can be replaced by slowness **S.** and the integration of the distance (x) will represent the forward operator, and can be written as a summation of small parts of discretized quintinum.

$$ti = \sum_{j=1}^{n} Si \times lij \qquad (2.3)$$

Where: (i) is the rank of the ray passes through j pixel, n total number of pixels.

The matrix of length of ray path (l_{ij}) representing the distance passed by each ray in each pixel can be replaced with the notation G.

$$d = G \times S \qquad (2.4)$$

$$G = \begin{bmatrix} l_{1l} & \dots & l_{1n} \\ \vdots & \dots & \vdots \\ l_{m1} & \dots & l_{mn} \end{bmatrix}, \qquad S = \begin{bmatrix} s_1 \\ \vdots \\ s_n \end{bmatrix}, \qquad d = \begin{bmatrix} t_1 \\ \vdots \\ t_m \end{bmatrix}$$

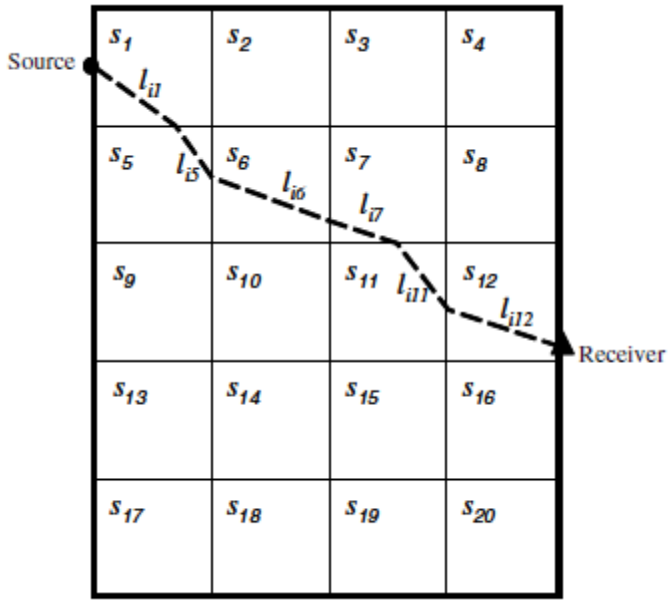

Fig (1.1): ray tracing from source to reciever according to LTI method in descitized model; by (Sambuelli et al, 2011)

2.4. Inversion:

The objective of the tomography is to characterize the Earth's model parameters (e.g velocity). The inversion step then is crucial to calculate and adjust the model parameter vector. An automated adjustment of the model parameter values with the objective of better matching the model data to the observed data will take place. An objective function to be minimized should be defined with an appropriate minimizing algorithm. Since most of gephysical problems are non linear problems, this nonlinearity should be taken into account when inverting seismic data. The inversion of seismic data is almost a non linear problem because of hetergonities and the application of Fermat's principle of ray transmission which states that the travel time is non-linear function of the velocity. It can be solved by linearize the problem to the travel time residuals and model parameter pertubations using discretization suitable to our observed data.This non linear problem can be linearized in case of weak nonlinearity or solved with global search methods in case of strong nonlinear problems.

2.4.1. Linearization:

According to Fermat principle we can consider a slowness of a non homogeneous mediu (curved route) as aggrigation of a linear (straight) path and some perturbation due to the heterogenity, mathmatically can be expressed as in formula ().

$$s(x) = s_0(x) + \partial s(x) \quad (2.5)$$

$$t = \int s_0(x)dx + \int \partial s(x)dx \quad (2.6)$$

But the quantity $\int$(s0(x))dx can be substituted with the traveltime (t0) of straight ray plus an excess time of slowness perturbation $\partial s(x)$ because of curved route due to heterogenity.

$$dt = t - t_0 = \int \partial s(x)\, dx \quad (2.7)$$

When we have a linear prblem of observed data (d), and model parameter (m) the inversion step, will solve the inverse problem by searching for model parameter best fits the observed data according to the formula().

But in case of linearization we solve the inversion problem by adopting model parameter perturbations adjustment (dx**)** to better satisfy the tavel time residuals (dt) of the observed data and forward calculated data.

$$dt = G \times ds \quad (2.8)$$

This misfit minimization traditionally carried out by a lot of mathematical algorithms developed specially for inversion schemes in last 40 years. Generally least-squares criterion is mostly used, and several methods originated from it.

2.4.2. Inversion algorithms:

In very fine descritized large problems, many of the elements of **G** will be zero in the sense that each ray path will usually only traverse a small subset of the M blocks. Two big catogaries of linearized inverse problem solvers according to (Rawlinson, 1996) are:

1- Backprojection methods: (ART, and SIRT), and

2- Gradients methods: (CG, and LSQR)

2.4.2.1. Backprojection Methods:

By refering to the backprojection techniques for solving the formula; they are depending on a row action method, by solving the problem along ray by ray (Rawlinson, 1996). Very well known tools are the Algebraic Reconstruction Technique (ART) and the Simultaneous Iterative Reconstruction Technique (SIRT). The ART is based upon the distribution of the traveltime residual of a certain ray to the unknown model parameters that the ray passed by; in an iterative way can be shown as in formula ().

$$mj^{k+1} = mj^{k} + \frac{tn^{k+1} \times lnj}{\sum_{m=1}^{M} l^2{}_{mn}}$$

Where:

- $t_n^{k+1} = d_n - t^k$, tn is travel time of nth ray, dn is the residual given by the difference of 0^{th} and k^{th} iteration,
- m^k_j is the approximation to the j^{th} model parameter at the k^{th} iteration,
- l_n is nth ray length

Although of the highly usage of ART before, especially in cross-hole models, and local earthquackes, but ART suffers from poor convergence properties like slow convergence and unstability (Rawlinson, 1996).

SIRT addresses some of the convergence problems regarded ART method by averaging model perturbations applied to each model parameter (cell) from all the rays that are influenced by the model parameter.

$$mj^{k+1} = mj + \frac{1}{R_j^k} \sum_{n=1}^{R_j^k} \frac{t_n^{k+1} \times l_{nj}}{\sum_m^M l_{nm}^2}$$

The SIRT method is popularly used in the inversion of teleseismic traveltime residuals, and in the inversion of reflection traveltimes for both velocity structure and interface depth.

SIRT and back projection methods in general converge slowly, although of their fast computation, this is at least partially due to the use of a kind of regularisation (spatial averaging). (Rawlinson, 1996)

2.4.1.2. Gradient Methods:

They are based on minimization of an objective function (relative deviation from initial model) defined already. This minimization is almost done using least square criterion. The objective function is defined as the difference between the real observed data and the synthetic calculated data produced by the forward modelling, and sometimes with another term of regularization or damping.

Let's consider the same subsurface body that we considered in backprojection methods with model parameter vector **m** and data vector **d** and so the traveltime residuals (**dt=t**calc-**t**obs) and model perturbations (**dm=m**calc-**m**0), the objective function (**W**) without regularization will be in the form:

$$W = dt - G(dm) \qquad (2.9)$$

By applying least square minimization iterativelly we can minimize the misfit function with repect to initial model m0 to an acceptable limit:

$$W = ||dt - G(dm)||^2 \qquad (2.10)$$

$$W = (dt - G(dm)).(dt - G(dm))^T \qquad (2.11)$$

And by equalizing the first derivative to zero:

$$\frac{\partial W}{\partial m} = 0 = G^T.G(dm) - Gdt \qquad (2.12)$$

The solution will be given according to the matrix equation, G is Jacobian matrix of derivative ($\frac{\partial m}{\partial t}$).

$$dm = (G^T G)^{-1} G^T dt \qquad (2.12)$$

$$m = m0 + dm \qquad (2.13)$$

Where: the operator $(G^T G)^{-1} G^T$ represents the generalized or psuedo inverse.

Usually the square matrix ($G^T G$) is ill conditioned; that means the observed data are insufficient to give a unique solution to the formula. One way to constrain the model is to introduce a coefficient giving waight to solutions near to a certain value in minimization procedure. This operation so called regularization. When we use a kind of regularization in least square solution, the approach called Damped Least Square **DLS**. (R. L. Nowack, and C. Li, 2009).

$$\begin{bmatrix} G \\ \varepsilon I \end{bmatrix} \delta m = \begin{bmatrix} \delta t \\ 0 \end{bmatrix} \qquad (2.14)$$

ε is a small, positive damping parameter. Solving this combined system using least squares results in

$$\delta m = (G^T G + \varepsilon^2 I)^{-1} G^T \delta t \qquad (2.15)$$

In most tomographic applications data residuals and model perturbation are given waights to overcome the shortcomings of regularization process (R. L. Nowack, and C. Li, 2009).There are several least square algorithms to solve a formementioned formula based on manipulation of generalized inverse used to solve the inverse problem to obtain model parameter.

Conjugate gradient Least Squares **CGLS** is one of iterartive methods commonly used to solve the inverse problem. It was introduced by Hestenes 1952 (Schleicher, 2018), and it is often used to solve large problems because it is faster than other algorithms. Each iteration a linear operator

and its adjoint are used. The reference model is the starting vector; and computation maight stop after few iterations (J.M.Lees, and R.S. Crosson, 1991).

CGLS solve the normal eqation generated from inverse matrix formula by conustructing a set of vectors that are mutually conjugated with respect to the square matrix of ray path product GG^T (Scales, 1987), (C. Thurber, and J. Ritsema, 2007).

The power point of CGSL is that the least-squares solution for **m** can be calculated with an efficient iterative algorithm based only matrix–vector and vector–vector products in a recursive manner; no actual matrix decomposition or inversion is involved. A super Efficiency can be obtained by the use of sparse-matrix methods, because the procedure does not involve matrix factorizations that can destroy sparseness. Sparse-matrix methods are particularly effective in tackling massive-scale tomography problems. (C. Thurber, and J. Ritsema, 2007).
CGSL came as a development to the steepest descent method which it uses only the gradient to minimize the objective function according to the equations bellow (W. Huang, H. Zhou, 2015).

The objective function:

$$W = \|Gm - d\|^2 \qquad (2.16)$$

By taking the gradient:

$$J_K = \nabla(W) = G(Gm^k - d) \qquad (2.17)$$

And the model will be updated as:

$$m^{k+1} = m^k - \alpha J_K \qquad (2.18)$$

Where the coefficient α can be achieved by standard quadratic line search or analytic solutions to reduce the value of objective function.
While the CG method updates the model in the conjugate direction of the gradient, the advantage is acceleration of convergence rate. After the first iteration using the gradient as it was used in steepest descent, the updated model will use a subsequent conjugate gradient.

$$m^{k+1} = m^k - \alpha_k S_k \qquad (2.19)$$

Where the subsequent conjugate gradient:

$$S_K = J_k + \beta S_{k-1} \qquad (2.20)$$

Where:

$S_0 = J_0$.

And the coefficient β can be calculated as:

$$\beta = \frac{J^T . J}{J_{k-1}{}^T . J_{k-1}} \qquad (2.21)$$

Paige and Saunders, (1982) developed an iterative method for the solution of large least-squares using Lanczos bidiagonalization technique; the Least Squares Quadratic Root LSQR method has a verry large common use. LSQR is a recursive procedure for solving the normal equations that is Identical and equivalent to CGLS with improvement of stability properties (C. Thurber, and J. Ritsema, 2007)

2.5. Sensitivity and Uncertainty analysis:

The inversion process is a numerical solution to a matrix formula involves of use of a pseudo inverse operator matrix with dimensions (m,n) of measurements and model parameters to be calculated (pixels of ray path), three probabilities exist relative to this dimension index:

1- Measurements graeter than the unknown model parameters (over determined problem) in which multiple solutions exist but can be constrained
2- Unknown model parameters more than measurements (underdetermined problem), where infinite solutions for the inverse problem.
3- Even determined problem when the number of measurements is equal to number of unknown model parameters to be calculated. This case is rarely happening.

Since most of geophysical problems are uneven, a non uniquness of the solution issue is essential, so it is obvious to investigate the solution non uniquness in order to choose the best resolution and the robust solution.

Basically reliability of the inversion solution can be measured by its coverage (depends on the geometry and parameterization), stability (defined as the sensitivity to small random errors), robustness (sensitivity to small number of outliers), and the resolution.

One of the common approaches for quality assesment is to apply synthetic resolution tests; otherwise, for linear inversion problems estimations of model covariance and resolution matrix can be made.

Regard the former one of non linear problems specially a continous property variance parametrization a test method is introduced to estimate the robustness of the solution by

conustructing a synthetic model using the same source reciever geometry to give a similar length scale to the original one. This similarity can measure the reliability. One of these well known tests is so called check board test.

For the second choice, a formal estimation of model resolution matrix is adopted. The concept of resolution matrixs comes from a fact that a generalized inverse product in inverse problem will not be an identity matrix, because it is not a true inverse, but it will be closed to the identity (Nolet, 2008).

If we considered the inverse problem matrix:

$$m = G^{-1}d \qquad (2.22)$$

Then we can obtain the following formula by multiplication with G.

$$G.m = G.G^{-1}d \qquad (2.23)$$

Since GG^{-1} should equal to identity matrix, then it can be taken as a filter or a miror to reflect the approachment of model parameter m to the true modelm_{true} for data that considered free of error (Nolet, 2008).

Another term introduced to overcome shortcomings of resolution matrix to faithfully represent the accuracy of the solution is the Posteriori model Covariance matrix (Nolet, 2008); this approach best fits small matrix problem where singular value decomposition is can bias the resolution especially in damping cases.

For an objective function with no smoothing term, the resolution matrix can be written as:

$$R = I - CM \times cm^{-1} \qquad (2.24)$$

I is the identity matrix,
C_M is a postiriori covariance matrix estimated by:

$$C_M = \varepsilon[G^T C^{-1}{}_d\, G + \varepsilon C^{-1}{}_m]^{-1} \qquad (2.25)$$

Cm is model covariance matrix, the diagonal elements of C_M indicate the uncertainty associated with each model parameter, and the diagonal elements of R range between zero and 1; in theory, when R = I, indicates a model perfectly resolved (N. Rawlinson, and W. Spakman, 2016).

3.Chapter three: Crosshole Seismic tomography

3.Chapter three: Crosshole Seismic tomography:

3.1. Introduction:

In cross-hole tomography, the first arrival travel times of the signals transmitted between souces and recievers placed in oppiste to each other in two boreholes are used to determine the seismic velocities in the region between these boreholes close to each other as it shown in fig (). (Imhof et al, 2010).

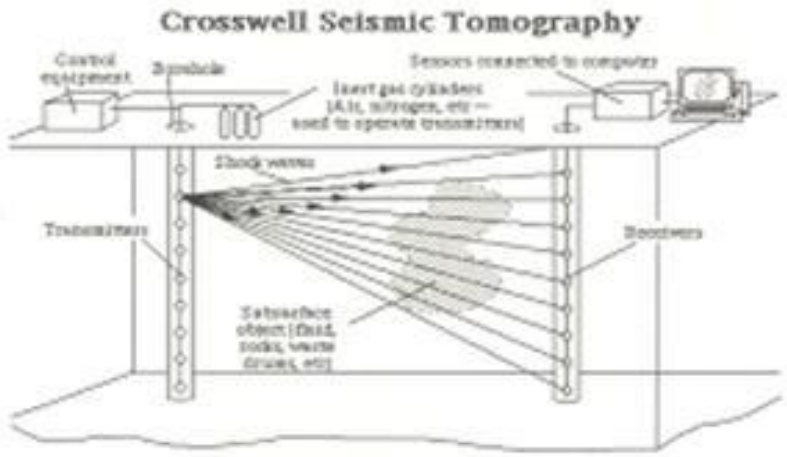

Fig (3.1): cross-hole tomography, by (Tojo- Vekas International, 2018)

It is the most case in seismic tomography similar to the origin of tomography techniques that invented by J. Radon in medical applications in the sense of the coverage and geometry (Nath et al, 2016).

Seismic tomography can be done in wide range of scales: teleseismic, global seismolgy, regional and local earth quake relocations. But when we come to use it in applied geophysics, specially explorational field, our scale will be in terms of hundreds meters, the cross hole geometry will thus best fits our scale.

In general the cross-hole tomography can be conducted either in parallel lines as two vertical boreholes or in orthogonal lines as vertical seismic profiling between a borehole and surface

(Gruber, 1998). Also the source reciever lay out can be placed each in bore hole or to swap both sources and recievers in both boreholes (Y. Rao et al, 2016).

3.2. Cross-hole Seismics applications:

The determination of the compressional (P) and/or shear (S) wave velocity of materials is one of significant advantages of cross-hole configuration in engineering and environmental fields, where the data can be used in analysis of soil mechanics, rock mechanics, foundation studies, and earthquake engineering; that need dynamic elastic moduli calculations (Cross hole seismic testing_geometrics.com, 2018). Cross-hole tomography can provide very detailed seismic p- and s-wave velocity information between closely-spaced boreholes, which can be used in:

- Bridge/dam foundation analysis.
- Insitu materials testing.
- Soil and rock mechanics.
- Earthquake engineering.
- Liquefaction analysis.
- Seismic ties to well data of Oil and Gas exploration.

3.2.1. Cross-hole in oil and Gas Industry:

In geophysical exploration, often we need to correlate some properties between boreholes. A number of tecniques has been proposed for this purpose, for example seismic ties to well data using a syntheic seismogram generated from well logs, and vertical seismic profiling VSP. Those tecniques gave opportunities to stratigraphic correlations and corrections to surface seismic surveys. Seismic crosshole will be an optimum tool and more accurate since it uses mostly first arrivals and borehole shots to model anomalies between boreholes. An inversion process is necessary after the pre-processing tasks of the survey data, to be able to assess some kind of geophysical model about the medium involved. The tomographic outcomes are typically, slowness or velocity distribution, and/or attenuation tomogram through the domain that permits to discover variations in it, which will lead to detect the model anomalies. Typically, crosshole survey is classified as a post drilling geophysical tool in contrast with predrilling surface geophysical surveys.Cross-hole seismic surveys used to resolve hidden layer velocity

anomalies that cannot be detected with conventional surface surveys. The results of crosshole data can be used multipurposely; for example, the seismic velocity results obtained may be used for stratigraphy characterization, fluid content analysis, deformation studies, or investigations concerning attenuation of strong ground motion.

A time lapse cross-hole survey is very useful in the entire oil exploration and production operations, especially for reservoir and geomechanics studies. Here are some cross-hole applications regarding oil and gas industry:

- Identification of high porosity zones between wells (where porosity is clearly related to seismic velocity)
- Locating well sites for infill drilling
- Monitoring enhanced oil recovery programs
- Structural and stratigraphic mapping of the reservoir and preparation of cross sections
- Monitoring reservoir dynamics such as movement of the gas cap or fluid contacts
- Improved reservoir characterization and modeling

3.3. Cross-hole tomography procedure:

Since the cross-hole is a tomography problem, the seismic inversion procedure will apply, Parameterization, ray tracing, inversion, and sensitivity analysis. In the next chapter we will investigate the inverse problem in cross-hole geometry in purpose of testing the reliability of grid manipulation represented by staggered grid method to enhance the image resolution.

Regarding the parameterization cell grid with constant velocity inside the cell often adopted keeping in mind straight ray theory, considering a homogenious medium. This approximation is well fits for depths greater than 10m as was demonstrated by (Imhof et al, 2010), unlike smaller depths, where stress-dependent anisotropy and heterogeneity are present producing ray bending, which complicate the inversion.

Most of popular inversion algorithms are commonly used for cross-hole tomography, such as the simultaneous iterative reconstruction technique (SIRT), algebraic, reconstruction technique (ART), and conjugate gradient (CG), and they are based on division of the subsurface area into a number of small constant-velocity cells and inversion of the time derivative matrix.

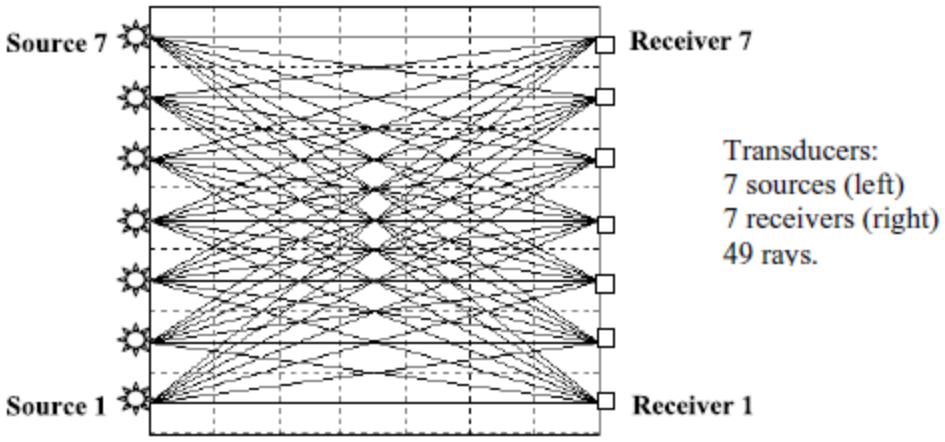

Fig (3.2): cross-hole straight raytracing in 49 cells using 7 scources and 7 recievers.

3.3.1. Resolution of seismic cross-hole tomography:

The resolution analysis is essential aspect to any inversion scheme. In cross-hole tomography, it has been found that the analysis of seismic and electromagnetic tomography data does not always give accurate and reliable results of the anomalous region. Cross-hole seismic tomography is an ill posed problem because of the relative distribution of sources and recievers which involves almost parallel rays that can increase the conditioning number (the ratio of maximum to minimum singular values) of ray path matrix according to (Imhof et al, 2010). In an ill posed problem the solution exists but is non unique and unstable. Ivansson in 1986 (Imhof et al, 2010) showed that non-uniqueness can be reduced to an acceptable level by adding more diverse data, and imposing constraints based on a priori information.The resolution, accuracy and the degree of distortion in the estimated images of course depend on the type of inversion algorithm used, the location of the anomalous zones between the boreholes, and the initial model parameters. Moreover, the ray path consist of only a small number of the total number of cells, the time derivative matrix will be generally sparse, causing difficulty in convergence when SIRT schemes is used (Nath et al, 1999). However, because two boreholes are so close to each other, the picking errors in traveltime data may have a greater effect than other tomography works, and the least-squares solution might be biased. In crosshole seismic data, the signal-to-noise ratio likely depends on the vertical offset between a source and a receiver (i.e vertical wells). The smaller the vertical offset is the more certain the observation should be,

because the overall attenuation will be smaller in general for a shorter raypath and hence the strength of the arrival increases and can be distinguishable (Rao et al, 2016).

In the next chapter we are going to apply the staggered grid inversion technique to seismic cross-hole tomography in purpose of increasing the reliability of the SIRT inversion and to obtain a better resolution levels and a reduction of non uniquness.

4. Chapter Four: 2-D cross-hole seismic inversion with staggered grid

4. Chapter Four: 2-D cross-hole seismic inversion with staggered grid

4.1. Staggered grid:

A lot of previous studies investigated ways of improving resolution, stability, and robusness of inversion algorithms with objective to get the highest degree of reliability. Some of these studies focused in smoothing and damping of an ultra fine discretization solution with introducing waighting coefficients (J.M.Lees, and R.S. Crosson, 1991). But some of them went in the direction of grid manipulation and adaptive meshing to minimize the mismatch of the data inversion and the observatin, because the damping and smoothing could bias the solution resolution (Arato et al, 2014).

One of meshing manipulation approaches is the staggered grid method.The use of a staggered grid to increase resolution and minimizing the inversion ambiguities and instability has been tested in a variety of disciplines as optical engineering, resistitvity (Arato et al, 2014), seismic applications (F. I. Louis, K. C. Makropoulos, 2005) and non-destructive testing (Sambuelli et al, 2011). In all these applications, the staggered grid approach has shown that a high reliability can be obtained to improve the resolution by shifting and merging a certain number of low resolution images. Arato et al, (2014) quoted that “Since the pixels can be equally resolved in every part of the image, the grid shift and the merging of the staggered images provide an enhancement to the spatial resolution by approaching several well-posed problems instead of solving one highly under-determined problem”.

The staggerd grid is based on the reiteration of a tomographic inversion using several different grid meshing schemes and averaging the model parameter values (slowness in our case) obtained from every inversion at the same given point. The different meshes are usually created by shifting the nodes of a selected mesh along vertical and horizontal directions. The inner cells within the imaging region can be shifted, yielding to a deformation of the cell size along the boundaries of the imaging region, while the total number of cells and the size of the cells not confining with the imaging region boundaries are preserved (Arato et al, 2014).

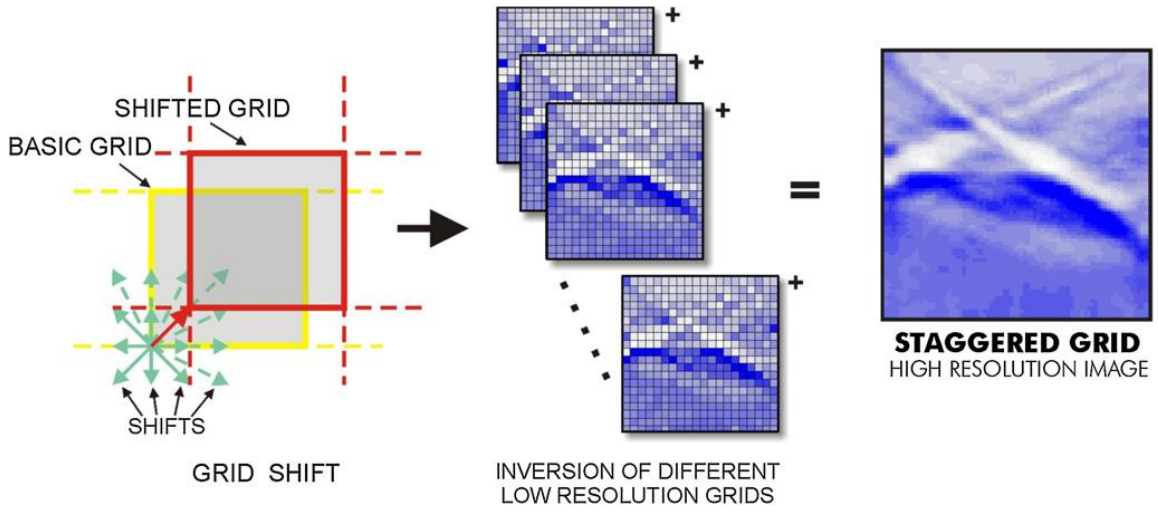

Fig (4.1): image enhancement using several coarse inversion grids with staggering, by (Arato et al, 2014)

Reasions behind the image enhancement by grid staggering is that the result is obtained by averaging the results of several inversions carried out on coarsely gridded models; this will contributes to limit the under-determination of the problem. Furthermore, the possibility to average the various solutions and to check the dispersion of the model parameter distribution cell-by-cell, this step can be useful in reducing the possible non-uniqueness of the solutions without imposing any a-priori information to constrain conditions, because, these priori informations, sometimes, are unknown (Arato).

(Luis et al, 2005) proposed a procedure for staggering seismic data in purpose of image enhancement, then applied by (Arato et al, 2014) in resistivity tomography which we are follow in this thesis. It can be summarized as follows:

1. A starting mesh grid should be defined. The grid can either be regular, irregular, or adapted according to the sensitivity distribution over the model; the problem is thus solved for the given mesh.
2. The nodes are horizontally and vertically shifted by a certain fixed amount, as ilustrated in fig (). Let's consider a regular grid within the imaging region, the horizontal and vertical cell dimensions are dx and dz. Then the final smallest size of the sub-cells after performing Nx and Nz shifts in the horizontal and vertical directions respectively would be.

$$Nx = 2 \times \left(\frac{dx}{sub_{size}} - 1\right) \qquad (4.1)$$

$$Nz = 2 \times (\frac{dz}{sub\_size} - 1) \qquad (4.2)$$

Where, the factor 2 means that the shift has to be performed along the same axis but in the two different directions, with a shift that is proportional to N*sub_size. The size of the elements remains the same in the central part of the imaging region, and in some cases the cell boundaries can coincide, even though the cells that conform to the boundaries of imaging region change their volume as a consequence of the shift.

3. The total number of newmeshes is N=Nx+Nz and the same traveltime dataset has to be inverted on each mesh. N should be not too large in order to avoid almost coincident meshes and to decrease the computationa time.
4. The final solution is obtained by averaging the model parameter (slowness) values of the cells having the same spatial coordinates in all the solutions.
5. This procedure is performed by resampling each staggered solution image to a new finer grid represented by sub-cells with dimensions of sub_size, keeping in mind a constant value initial parametrization. The resampled i-th cell has (dxi/sub_size) sub-cells in the x direction and (dzi/sub_size) sub-cells in the y- direction.
6. A variance measure of slowness value at each sub-cell is calculated.

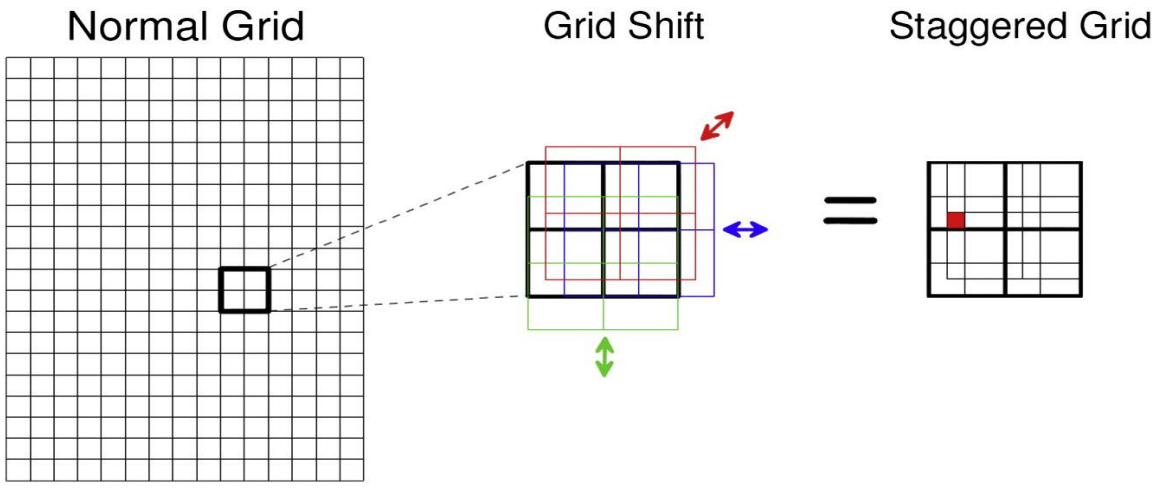

Fig (4.2): grid shifting in horizontal and vertical axes, and sub_size pixel, by (Arato et al, 2014)

4.2. Staggered Grid Random Tomography software (SGRAT):

Seismic tomography data inversion matlab software based in tomotool software and it is developed by: A. Godio and L. Sambuelli in 2011 to process seismic cross-hole data using Simultaneous Itrative Reconstruction Teqnique (SIRT) and Conjugated Gradient as inversion algorithims with regular rectangular grid. SGRAT has the ability to generate synthetic models and process real field data set to be inserted in migratom format with capability to use either regular or random parameterization. SGRAT uses rectlinear ray tracing to solve the forward model, SIRT, and CG for inversion in iterative operation. The user interface contains five principle commands: “File” to manage the input and output, “Forward model” to generate and manage synthetic models, “CG inverion” use of conjugated gradiend inversion method, “SIRT inversion” for SIRT algorithm, and finally “Display”to show the outputs like velocity map and statistics.

4.2.1. Parameterization and Ray tracing:

SGRAT has the capability to set the initial model according to the user needs. In case of model generation, the user can put an initial model by defining the max velocity, min velocity in a normlized (divided by 1000) or (km/s units), but the distribution should be inside the matlab script of set model function. There are options of creating either a random model parameter distribution or a regular one. For raytracing related to the iterative operations of inverse algorithm however it was CG or SIRT, the initial slowness is set as a mean value inserted by the user as input parameter in case of CG inversion, and it is calculated as a mean of aparant velocity from the rectlinear ray path and the corresponding traveltime. The ray tracing used in the SGRAT software is straight rectlinear ray path to simplify the inverse problem; this assumption is acceptable in a very small velocity variance for depth more than 10 m (Imhof et al, 2010).

4.2.2. Inversion algorithms:

The software is designed to excute inversion operation using either Simultaneuos iterative reconustruction technique (SIRT) or Conjugate Gradient method (CG).

- **DSIRT inversion:**

A damped version of SIRT invented by Trampert and Leveque in 1990 (Sambuelli et al, 2011) is used in the inversion using a set of formula's to be clarified below; the slowness vector estimation S_{q+1} after q iterations can be written as:

$$s^{q+1} = [(1-\theta^2)I - A^{-1}G^T B^{-1}G]S^q + A^{-1}G^T B^{-1}t$$

$$A = diag\left(\mu_1 + \sum |G_{ij}|^{\alpha}\right)$$

$$B = diag(\mu_2 + \sum |G_{ij}|^{2-\alpha}$$

Where:

- **α***:* is a weighting exponent has a range from 0 to 2;
- μ1 and μ2: are two positive numbers that allows for inserting physical *a priori* information in the solution and,
- ϑ^2: is a damping constant comparable to the one used in a damped least-squares algorithm.

It is then possible to define both the data resolution matrix **D** and the model resolution matrix **R** .

$$D = G(G^T B^{-1}G + \theta^2 A)^{-1}G^T B^{-1}$$

$$R = (G^T B^{-1}G + \theta^2 A)^{-1}G^T B^{-1}G$$

The data will be filtered inside the inversion code before imposing the inversion algorithm to stabilize the output by eleminating the far extremist rays and cells in three criterions by taking following procedures:

Firstly the average of numbers of cells intersected by each ray calculated with the standard deviation. This standarad deviation is weighted with a certain factor **k1** range from (1-4) inserted

with inversion inputs, then the rays less than absolute value of mean substracted by the weighted standard deviation will be eleminated. Secondly,the travel times residuals (tobs-tcalc) average calculated considering apparent velocity of the straight path between source and reciever, then discarded rays of reiduals out of the range of absolute difference of the average and the **k2** (same as **k1**) times standard deviation. Finally the total length of rays passed through the pixel was calculated with the average and standard deviation in a step to eleminate the cells out of the range of average and **k3** times standard deviation.

The first stopping criterion is simply the maximum number of iterations, while the second is aminimum threshold on the difference between the root mean square residuals (rmsr) defined as:

$$rmsr = \sqrt{\frac{\sum_{i=1}^{m}(t_i{}^{calc} - t_i{}^{meas})^2}{m}} \qquad (4.3)$$

- **Conjugated Gradient inversion:**

The algorithm used is the conjugate gradient inversion algorithm that introduced by Hestenes and described by (Scales, 1987) the same of that described in gradients methods in chapter two.

4.3. Run Flow chart:

The procedure to run SGRAT is illustrated as in the flow diagram as in shown in fig (4.3) and fig (4.4)

❖ Forward modeling flow chart (synthetic data generation):

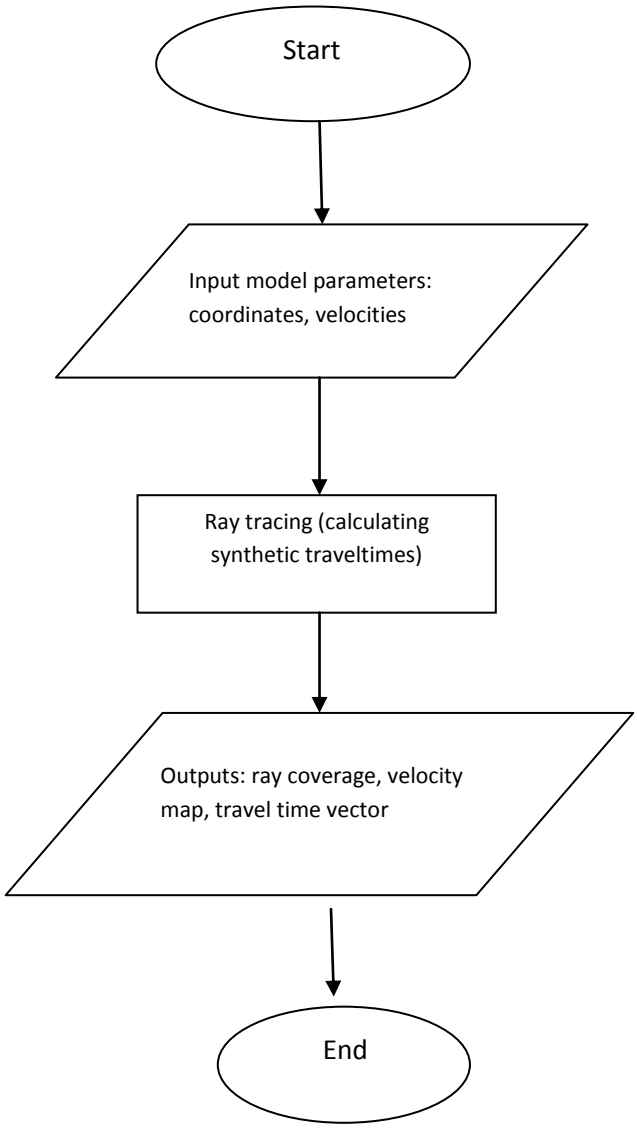

Fig (4.3): forward modeling flow diagram

❖ Inversion flow chart:

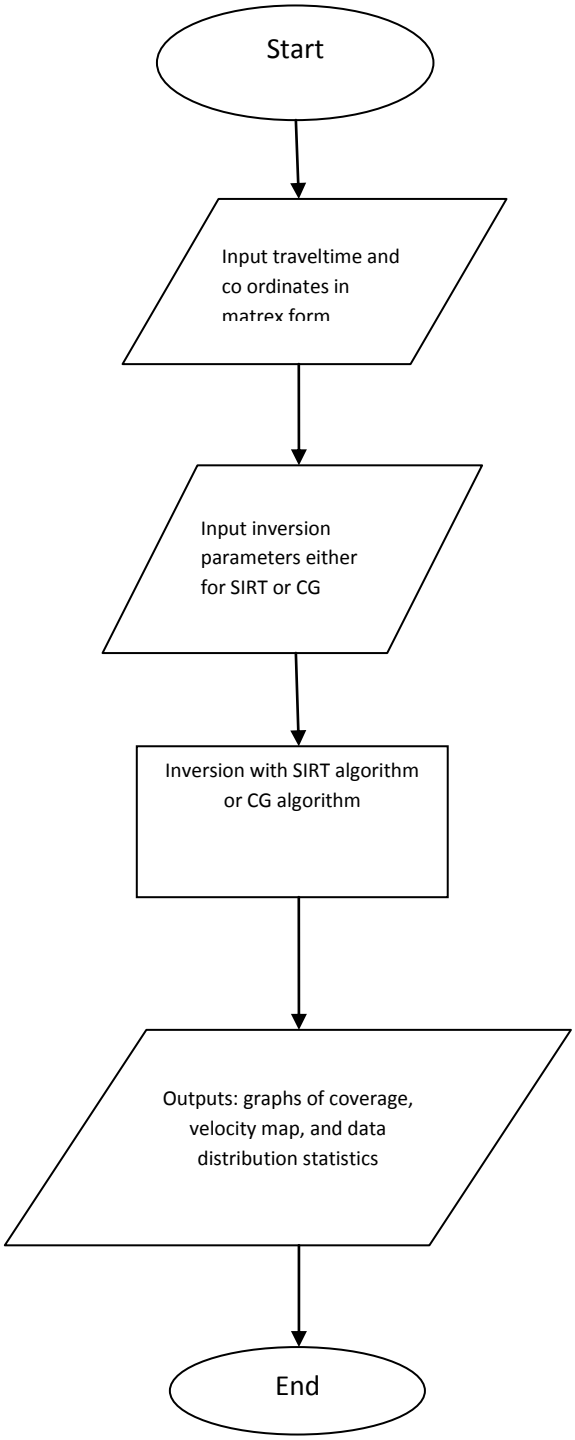

Fig (4.4): illustrating inversion flow diagram

4.4. Modifications and improves of some functions of SGRAT:

1- Solve some erorrs of the command “set_model” forward modeling command. The function (reshape) which is used to redistribute the values of velocity have been input to the model according to the cell matrix with dimensions (cx*cz).

2- Recovering some errors in ray tracing for CG inversion and adding plots of ray coverage and velocity map to the inversion function to be displayed automatically

3- Insert new script file to make the window of inserting SIRT inversion parameters more comfortable and visible enough.

4- Including some plots of traveltime data stastistical results: plot of total length per cell (spatial coverage), ray density (total rays passed through the cell), in SIRT inversion and conjugated gradient.

5- Some plots in both SIRT, and CG inversion regarding statistics located in function (Display) are activated and improved.

6- Test the SIRT inversion algorithm before and after staggering on two sets of synthetic data and a real field dataset, and discusing the inversion outcome reliability.

a) b)

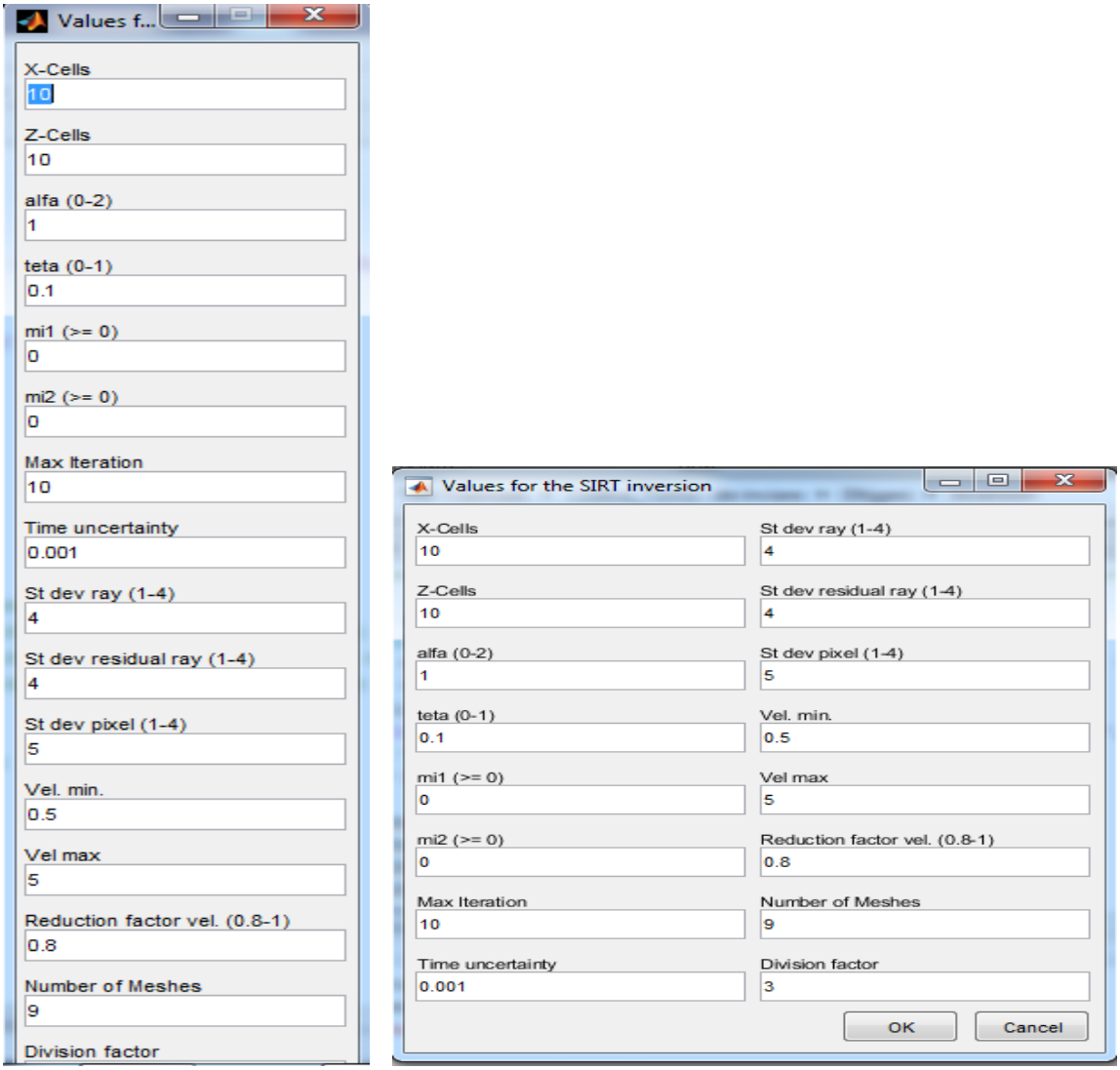

Fig (4.5): the input screen of SIRT inversion parameters input, a) before and b) after.

4.5. 2D seismic cross-hole inversion using SGRAT:

4.5.1. Application to synthetic data:

A synthetic model created using the modeling tool in forward subcommands.Travel time datasets generated by the enrty of shots and recievers coordinates; maximum, minimum, and background velocities are defined. A rectangular area of length 20 m, width of10 m; 29 shots and 29 recievers is considered in a way such that 19 of them along the length and the rest are

along the width like as shown in fig (4.6) and the recievers are in the front side to the source in same elevation or distance. The anomaly is considered to be the higher velocity in the center with an inverse (L) shape with a value of 3 km/s and the background is 1 km/s, fig (4.7). The forward grid is taken as each pixel equals to $1m^2$.

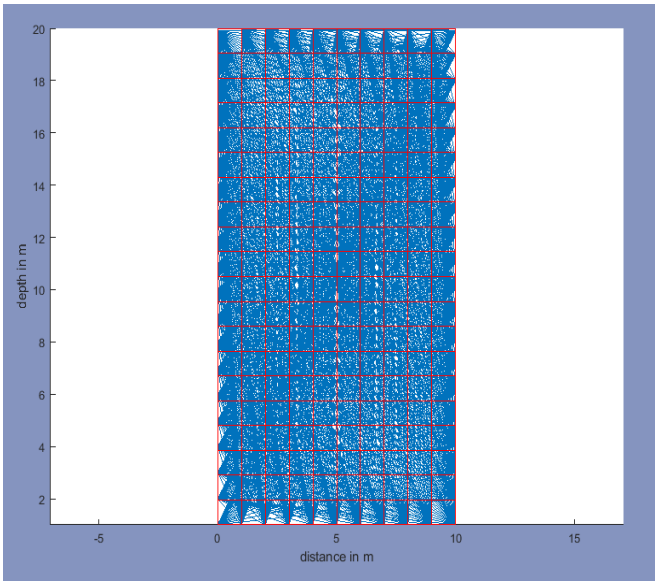

Fig (4.6): Synthetic model ray tracing coverage

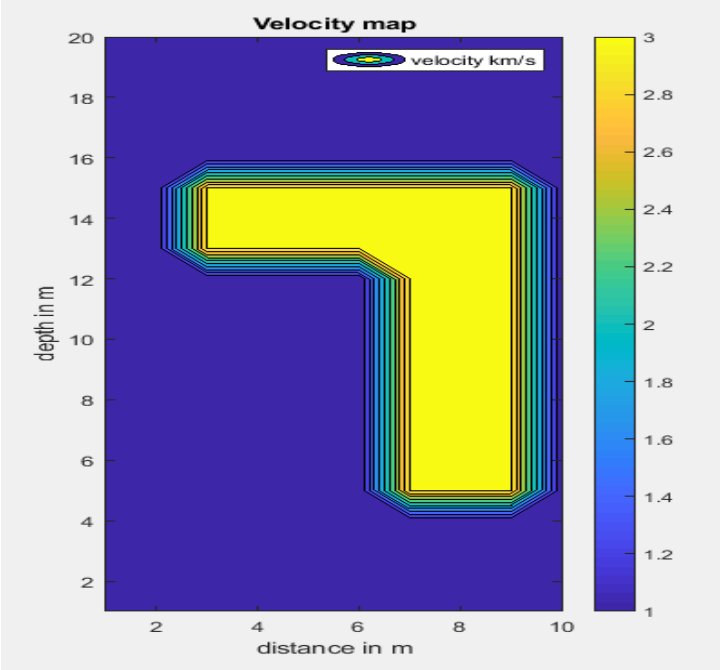

Fig (4.7): synthetic model includes back ground velocity (1km/s) and velocity anomaly (3 km/s)

SIRT Inversion parameters to be inserted:

Table (4.1): input parameters for SIRT inversion

parameters	value
x-cells	10 (15 in case of fine grid)
z-cells	10 (30 in case of fine grid)
A	1
Θ	0.1
μ1	0
μ2	0
Max iterations	30
Time uncertainity	0.001
K1	2
K2	2
K3	2
Vel min	0.5
Vel max	3
Reduction factor	0.8
Number of mishes	2
Division factor	2

We made another SIRT inversion test with a finer inversion grid for the same model to compare results of staggered inversion to the fine inversion. The input parameters are remained the same except the number of (x) cells (=15) and (z) cells to be (30).

4.5.2 Application to Real field dataset:

4.5.2.1. Location and Data aquision and processing:

The real field data are open source data downloaded from internet from the UTAM (Utah University consertium of Tomography and Migration Modeling) website, and they are chosen although they are not a cross bore-hole tomography, because of their similarity to the cross hole configuration, that the ray path from source to reciever can be considered direct with reference to the degree of scale (tens of meters depth, hundred and fifty length) according to (Hanafy et al, 2012). The data are collected in the context of testing and validating the time reversed mirror scheme for locating trapped miners and its high-resolution and super-stacking properties, the

experiment was carried out on 21 May 2009, it was along a cliff in Moab, Utah by a group of researchers from geophysics dipartment of university of Utah.

The fig (4.8 a) shows a cross-section sketch of the site of the experiment, and source-receiver geometry, while the other fig (4.8 b) shows the real cliff. The recievers spread layed out on the top of the cliff at a height of about 60 m and the array is 45 m away from the edge of the wedth side of the cliff. This means the straight line distance between the sources and receivers is 75 m or greater. Fig (4.8 b) is a picture taken at the experiment site.

The seismic source was a sledge hammer at the bottom of the cliff. The recording array constructed from 72 receivers with a receiver interval of 2 metres; 21 shots with a shot spacing of 4 metres with a purpose of generating the seismic data to test the scheme of locating seismic sources with time reversal mirrors. During the acquisition of the data, multiple strikes of the hammer sources at the same location have been carried out and then these traces stacked together to reduce noise and amplify the signal. In this test, the data are acquired with a very high signal-to-noise ratio. The frequency band of the field data is estimated to be from 8–204 Hz. The gathers are preprocessed with a band pass filter (8–204 Hz) and amplitude normalization. Then the gathers are trace normalized to correct the differences in geophone coupling, where the amplitude values of each trace are divided by the maximum absolute amplitude of that trace. In this field test, the P-wave velocity is estimated from the collected data to be 1364 m/s and the peak frequency of the data is 42 Hz to give a dominant wavelength of 16.2 m; thus, the Rayleigh resolution limit is computed to be 4.3. The data are recoreded in many formats (segy, matlab … etc), but in our case the matlab format was adopted and processed in a matlab code created for this purpose.

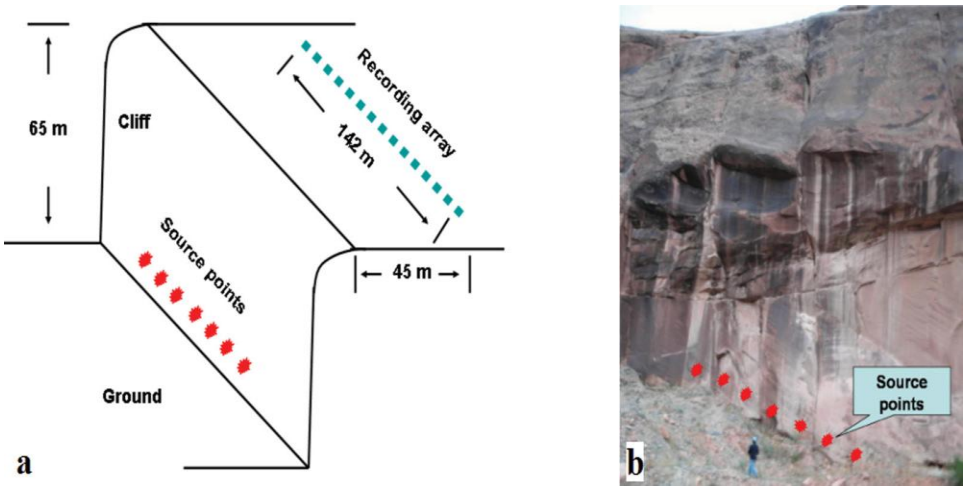

Fig (4.8) shows the location an sketch of the experiment, by (Hanafy et al, 2012)

4.6.2. Travel time picking:

Since the data are in signal digitalized sampled format (matlab file), a picking step is necessary to pick travel times (first arrivals), which are the principle input of the seismic traveltime tomography. A matlab code has been created to pick the travel times manually using the mouse from a seismic section as in fig (4.9).

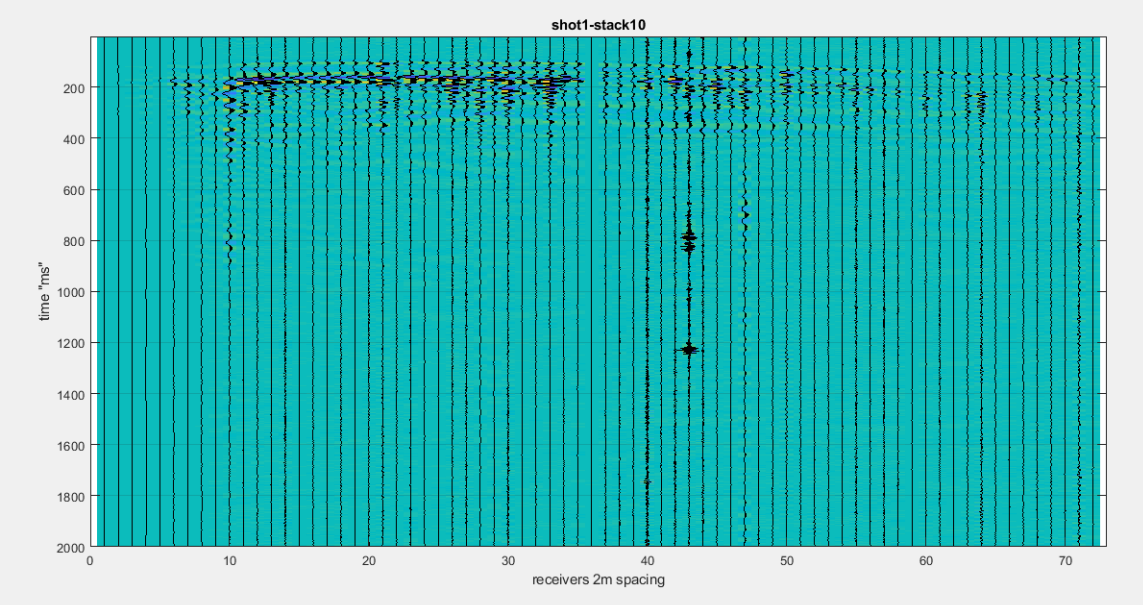

Fig (4.9): Seismic cross section of raw data collected in Utah University

A matrix of the picked travel times associated and their coordinates created in a text file format to be used in the software after convert it in a migratom file with extension (.tt).

Software setup: the software set up by run the basic code tomotool to open the interface and the input data have been inserted according to the inversion method.

By asigning values of inversion parameters through the inserting window, they should be reasonable and care of spatial resolution and mathematical solution capability (not under-determined). The product of the number of cells in (x) direction and (z) diretion will define the dimension of model parameter vector (m) (slowness vector) should be less than the number of measurements in the traveltime input file (n). The inversion took place with a coarse grid (10*10), this will give a pixel dimensions to be (14.2*7.5) m^2, and then staggered grid applied with a random and regular mesh. Another SIRT inversion scheme carried out in fine inversion grid (30*15) yields a regular (4.73*5) m^2 cell diemension for comparison purpose. The coefficients values have been taken equal to be 1for α and 0.1 for θ with null value for a priori information coefficients $\mu 1$ and $\mu 2$. The stopping criteria values are the maximum iterations (40 times) and time uncertainity (the acceptable error =0.001). Minimum and maximum normolized velocities have been intered with values: 0.5, and 3 respectively. We used 2 meshes for staggered grid inversion with step about 2 m in velocity map resampling and reconstruction. We got the outputs in terms of figures and numerical values for traveltime residuals saved as a text file.

SIRT inversion input parameters: Data are inserted as in shown in table (4.2).

Table (4.2): real data SIRT inversion input parameters

parameter	value
X - cells	**10 (30 in fine inversion)**
Z - cells	**10 (15 in fine inversion)**
α	1
θ	0.1
μ1	0
μ2	0
Max iterations	40
Time uncertainity	0.001
K1	2
K2	2
K3	2
Vel min	0.5
Vel max	3
Reduction factor	0.8
Number of mishes	2
Division factor	2

4.6. Results and discussions:

The typical results of the inversion are: plots evaluate coverage, numerical indicators of accuracy and number of iterations and velocity maps. The plots of coverage includes the ray tracing coverage, in addition to messures according to the statistics discussed above in DSIRT formulation and discard of radical values , this measures are spatial coverage plot represents the total length of rays pass through each pixel, and ray density which it shows the number of cells in each pixel. This statistics also supported with numerical values displayed in the work space and saved into a text file document.

The resolution will be discussed with different Key Performance Indicators (KPIs), some applied to the single mesh inversion, and some for the average values of these staggered mesh produced from these single meshes. For those regards the single mesh inversion, we have plots of diagonal of the data resolution matrix, and diagonal of the model resolution matrix, in addition to comparisons between initial data residual values and final residual values using plots of the residuals of each ray, and a histogram of the initial and final residual values . Finally the

square root of the residuals calculated and plotted against number of iterations, and this KPI is used to evaluate the outcome of staggering along side with velocity maps.

4.6.1. Results of Synthetic Model inversion:

The initial mesh spatial coverage and ray density plots:

These plots show a dense coverage in the middle region of the model coincide with right angle diagonal thanks to the geometry and distribution of source and recievers, which it yields to a non equal resolution, the resolution is high along this diagonal, and get lower far from the diagonal, this will give us an idea about the amount of information and details can be obtained.

Fig (4.10) and fig (4.11) show the coverage for coarse and fine grids used.

a) b)

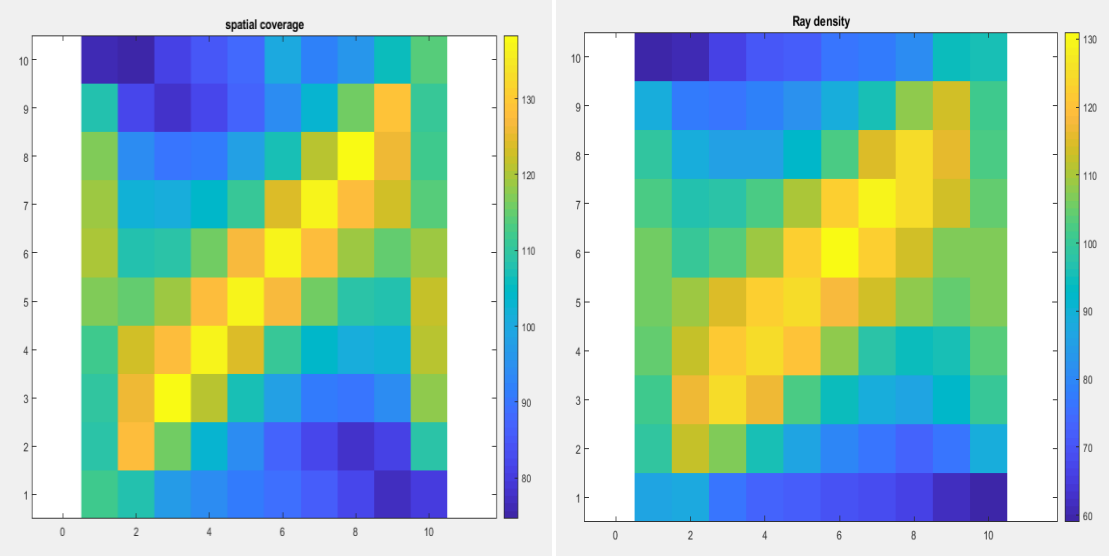

Fig (4.10): coarse grid SIRT inversion on synthetic data, a) spetial coverage, b) ray density

a) b)

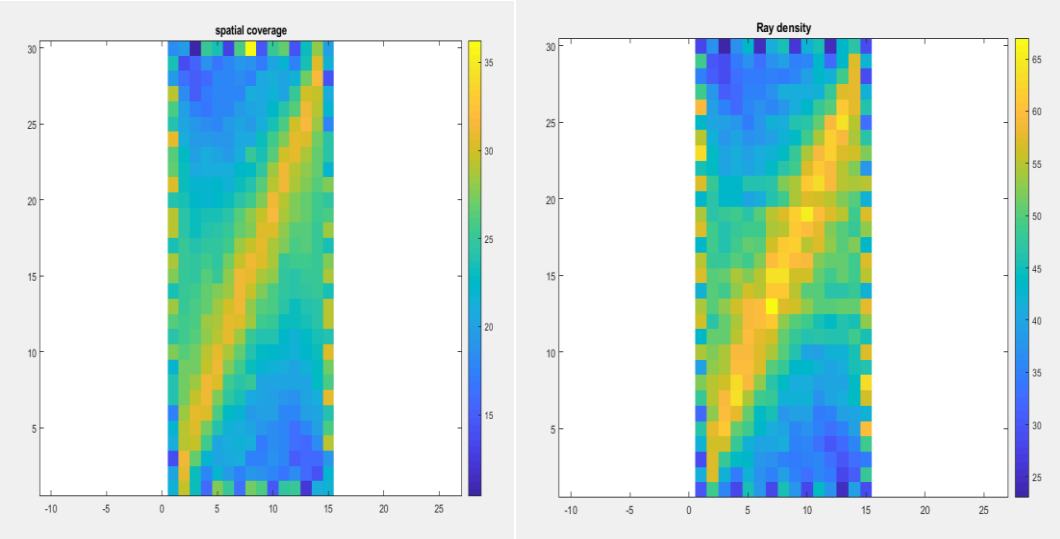

Fig (4.11): fine grid SIRT inversion on synthetic data. a) spatial coverage, b) ray density

- **The results of SIRT inversion:**

Table (4.3): results of SIRT inversion on synthetic data

parameter	Coarse (10*10)	Fine (15*30)
Rays eliminated (attraversing less cells)	41	41
Rays eliminated (high residuals)	44	45
Cells eliminated (less rays passed through the cell)	3	10
Fattore di incremento v<vmin (1<-<2)	1.2	1.2
iterations	16	16
Error percentage (sqmres%)	%10.54	%9.80
Final sqmres value	1.3267	1.1765

- **Diagonal of resolution matrix plots:**

Those plots represent the resolution as explained before in the formulation of DSIRT inversion algorithm. They confirm the coverage estimation about the details can be obtaind with a better resolution in the middle of the image as in shown in model resolution matrix with maximum value approaching 50% and almost centered arround the average 45% with a very low deviation.

The same thing can be said to the data resolution matrix, except in the value of the resolution which it ranges from 0.03 to 0.13.

Fine grid inversion gives better data resolution matrix and model resolution matrix than the coarser grid, can be shown clearly in fig (4.12), fig (4.13) and fig (4.14).

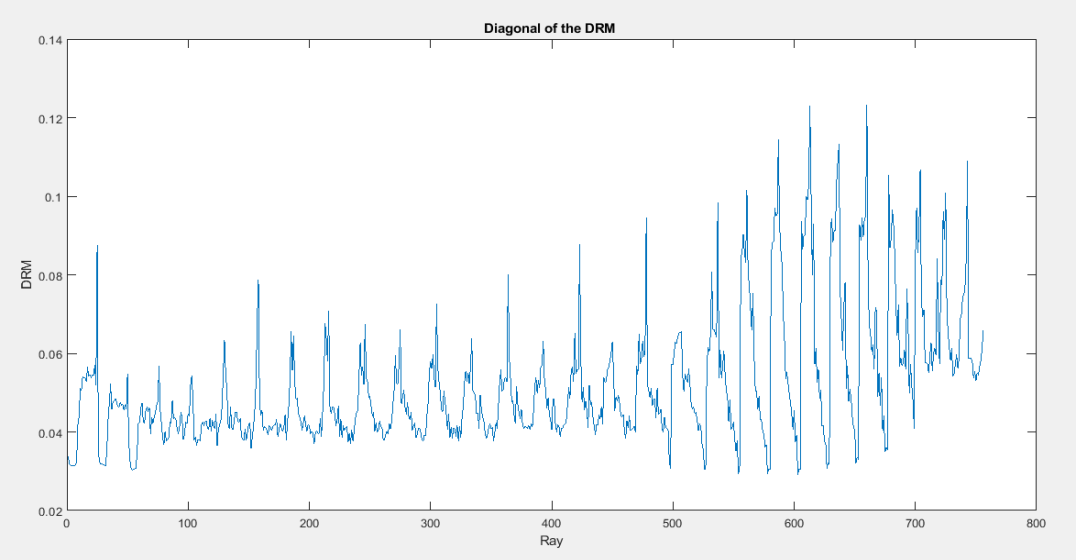

Fig (4.12): Synthetic model SIRT inversion in coarse grid; Diagonal of DRM

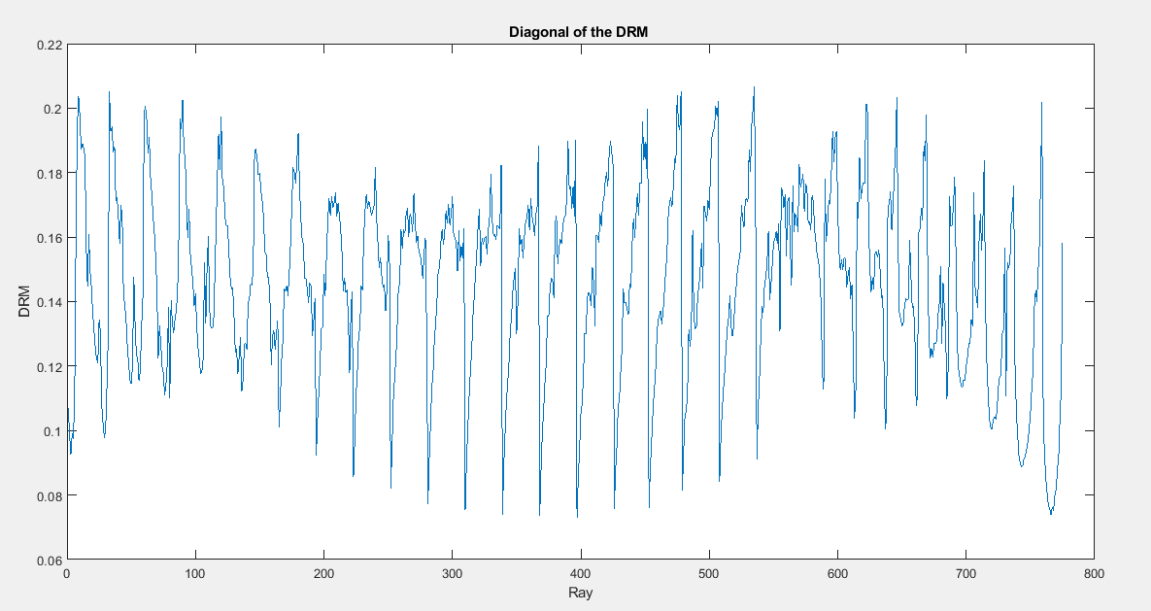

Fig (4.13): Synthetic model SIRT inversion in fine grid, Diagonal of DRM

- Model Resolution matrix:

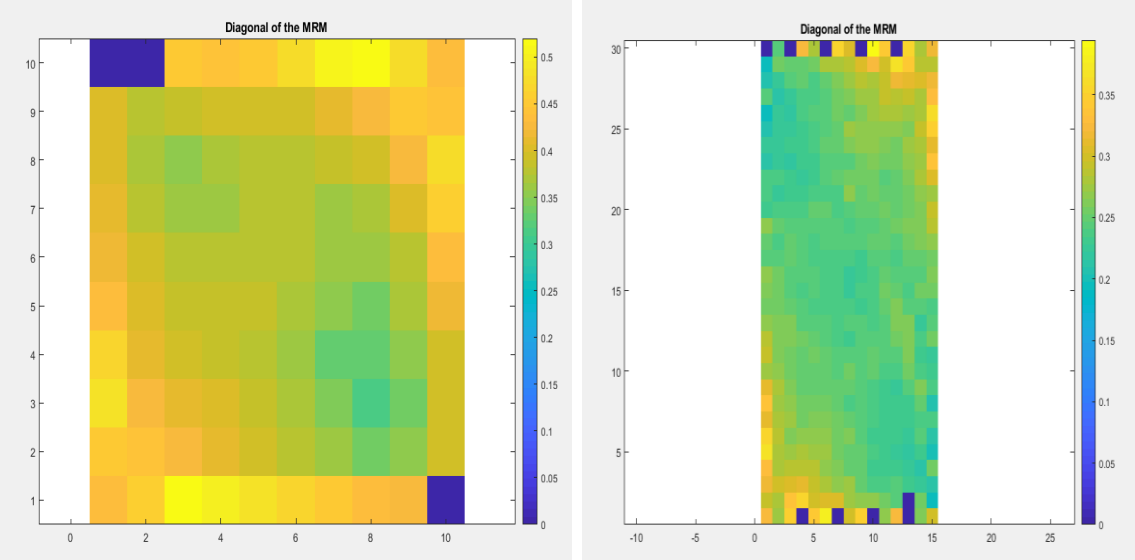

Fig (4.14): synthetic data SIRT inversion diagonal of MRM, a) coarse grid, b) fine grid

- **The residuals comparison plot and evolution of rms of residuals:**

The residulas mean square root value reduced from an initial value of 1.7 ms to 1.2 ms in 16 iterations for both coarse and fine grids, satisfying the second stop criterion in 16 iterations out of 30 iterations proposed. This residual root square gives an error percentage of 10.5 for the coarse grid and a bit better in fine grid with 9.8 as shown in table (4.3).

Fig (4.15) shows how is the difference between the results of first and last iteration which it can be considered reliable results for some extent, residual values are in ms.

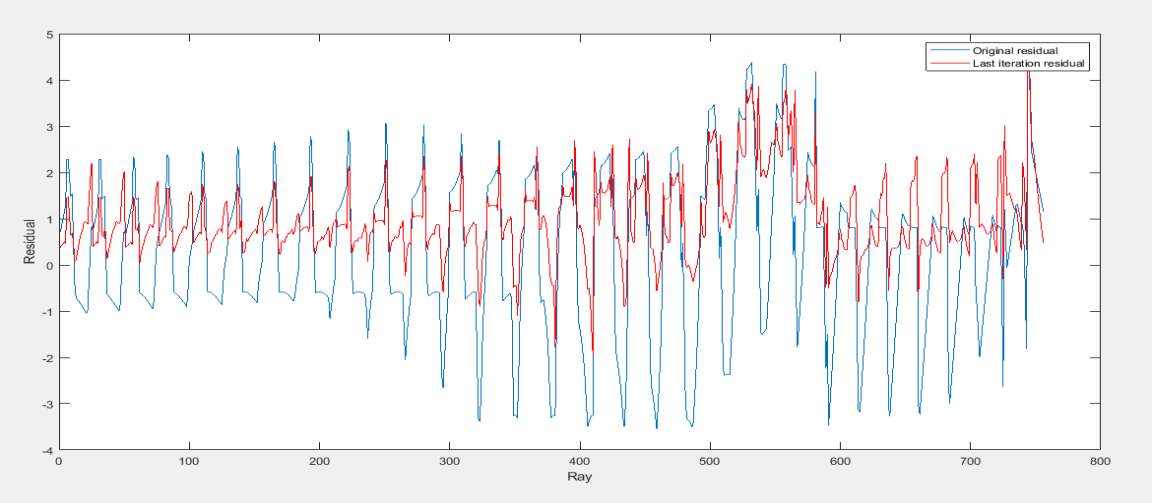

Fig (4.15): syntheic model SIRT inversion in coarse grid; plot of initial and final residuals

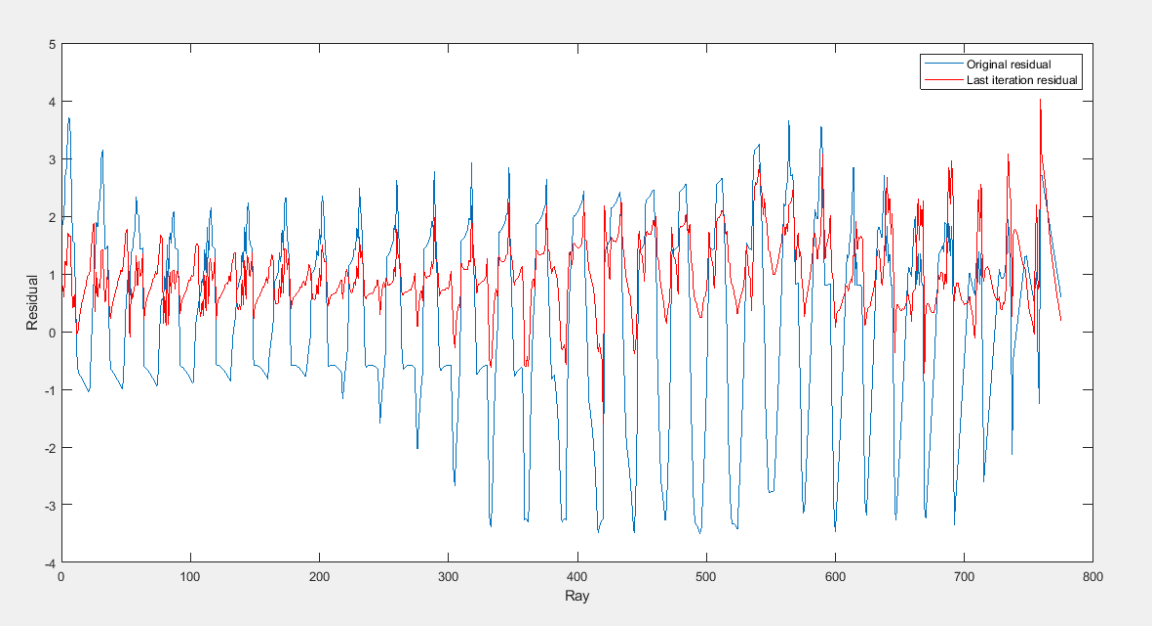

Fig (4.16): synthetic model SIRT inversion in fine grid; plot of initial and final residuals

a) b)

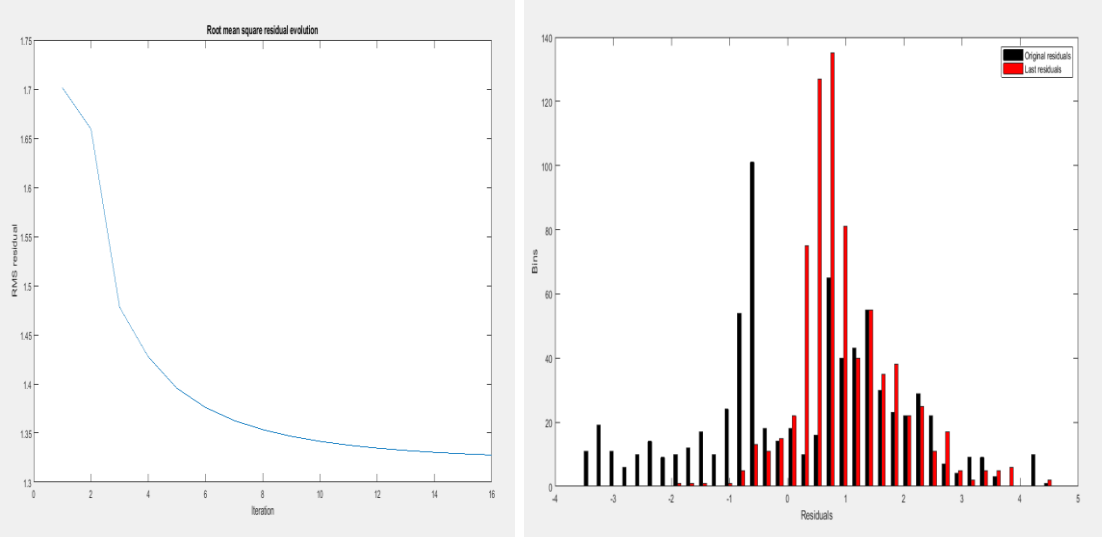

Fig (4.17): Synthetic model SIRT inversion in coarse grid; a): rms of residuals evolution. b) residuals histogram

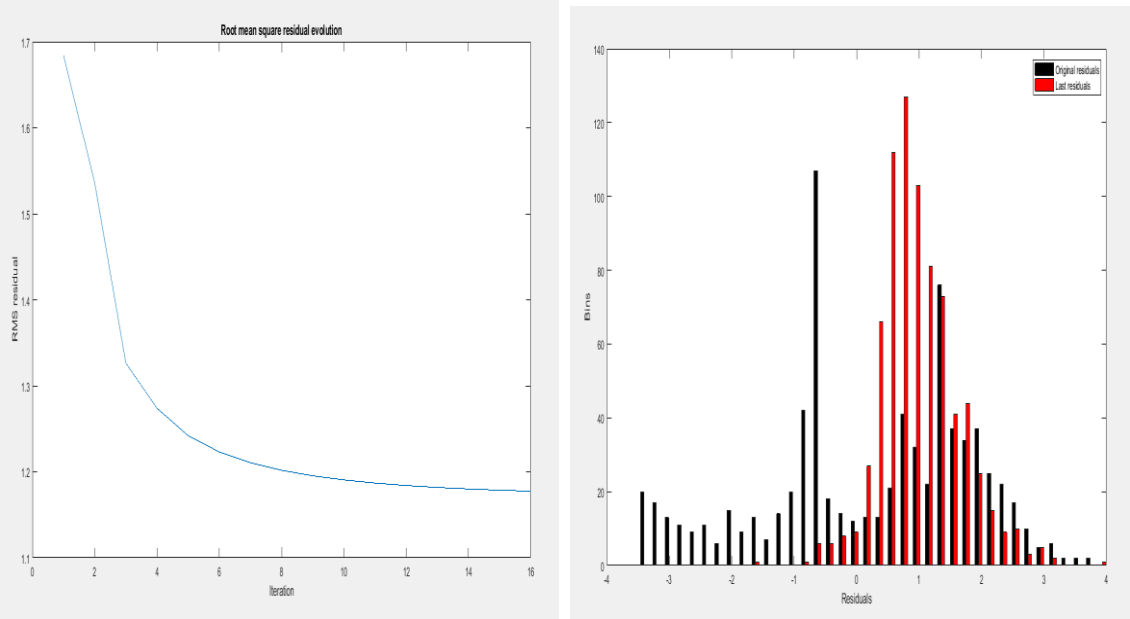

Fig (4.18): Synthetic model SIRT inversion in fine grid; a): rms of residuals evolution. b) residuals histogram

- **Velocity map of sirt inversion:**

The velocity map fig (4.19) and fig (4.20) reflects the true model in geometry and position of the velocity anamoly in the centre in a gradual way unlike the sharp initial model, but the velocity values ranges from 0.5 to 2.5 km/s at maximum which it is lower than the value of the true model anomaly value.The fine grid inversion shows a wide area of velocity anomaly with a same value as coarse grid.The shape of the anomaly generally reflects the initial model but more chaiotic in case of fine grid.

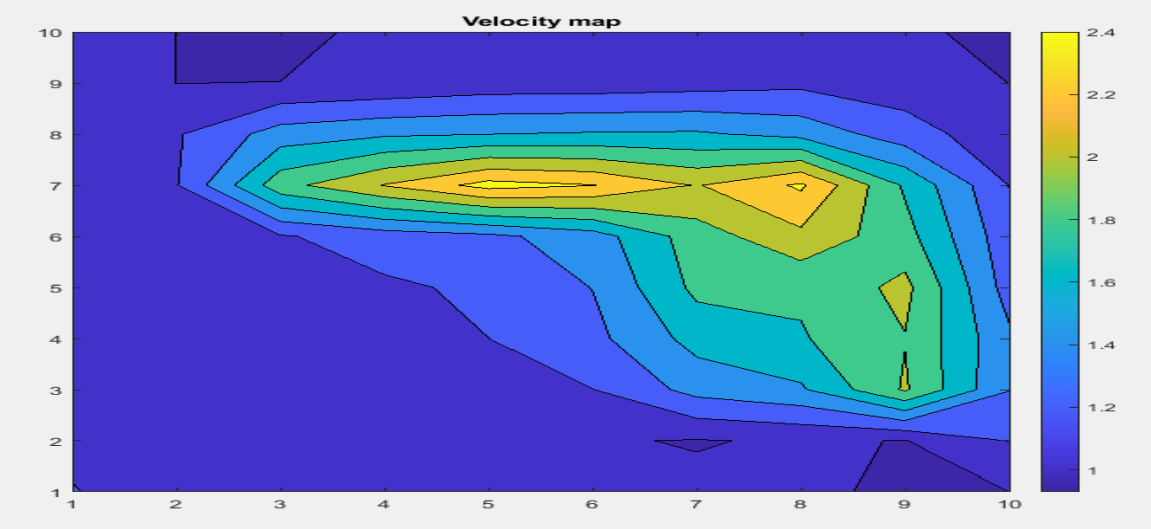

Fig (4.19): Synthetic model SIRT inversion in coarse grid; velocity map

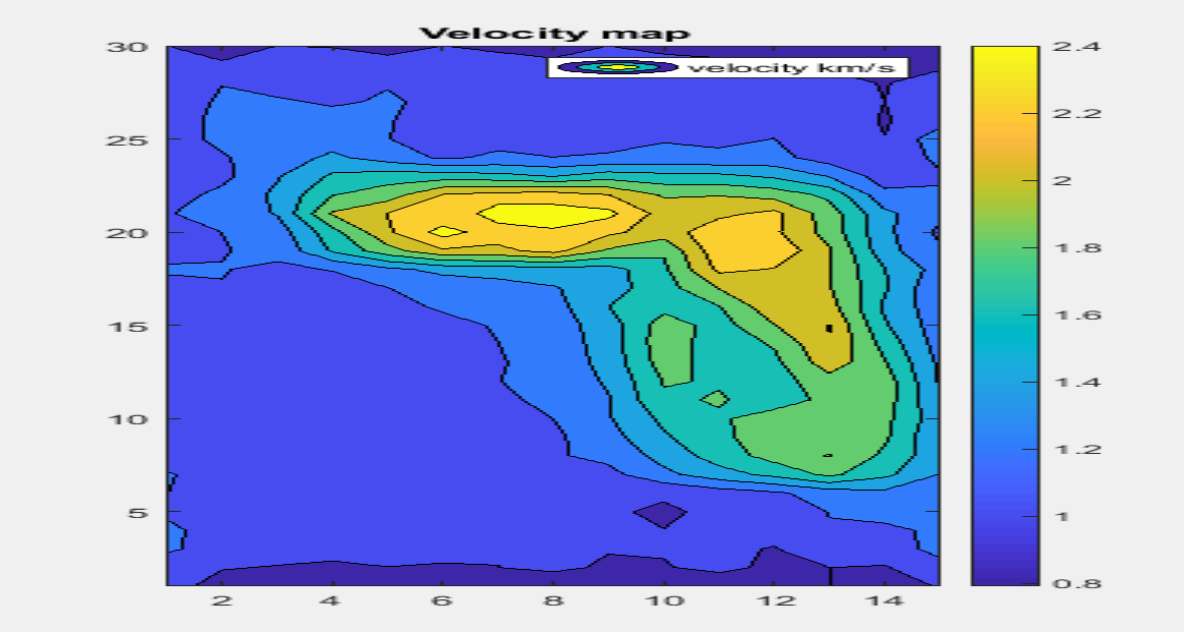

Fig (4.20): syntheic model SIRT inversion in fine grid; velocity map

- **The staggered grid inversion results:**

Results after random and regular mesh staggering on 2 meshes with division factor 2 units:

Table (4.4): syntheic model SIRT Staggered grid results

parameter	Random staggered	Regular staggered
Rays eliminated (attraversing less cells)	46	33
Rays eliminated (high residuals)	44	44
Cells eliminated (less rays passed through the cell)	0	4
Factor of increment v<vmin (1<-<2)	1.2	1.2
iterations	16	16
Sqmres % (error percentage)	%9.7487	%10.0592
Final sqmres value	1.3267 ms	

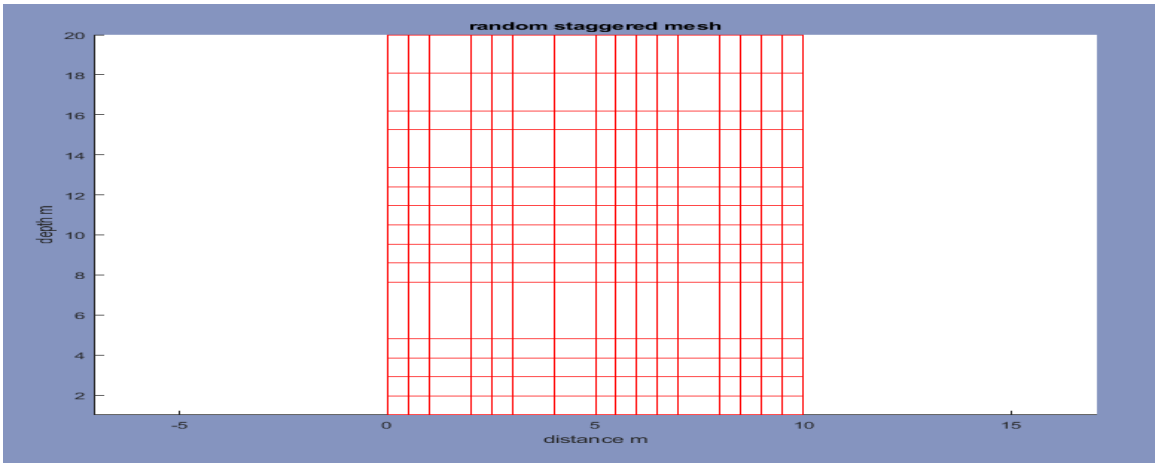

Fig (4.21): Synthetic model SIRT staggered inversion; irregular mesh.

The velocity map after staggering:

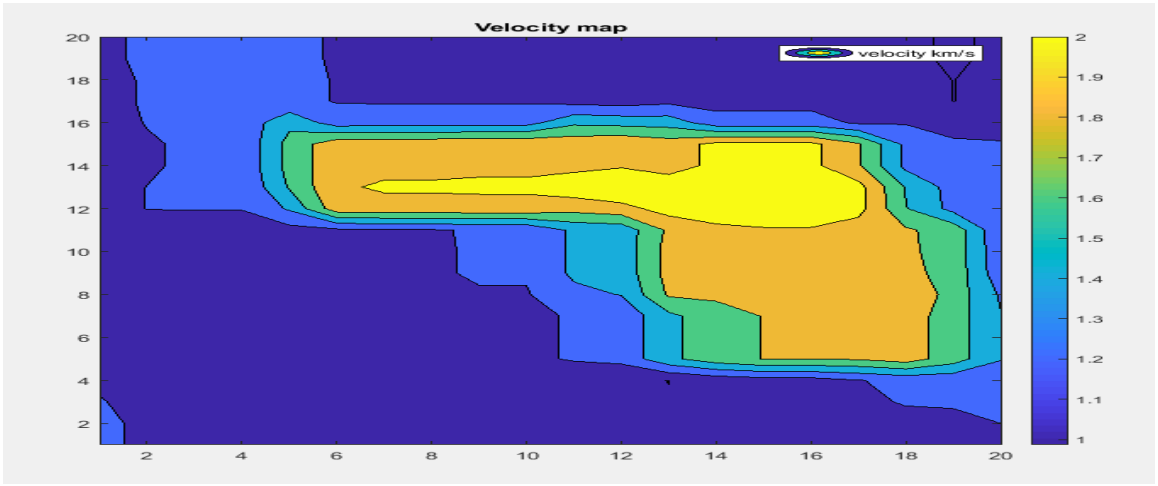

Fig (4.22): Synthetic model SIRT staggered inversion in irregluar (random) mesh; velocity map

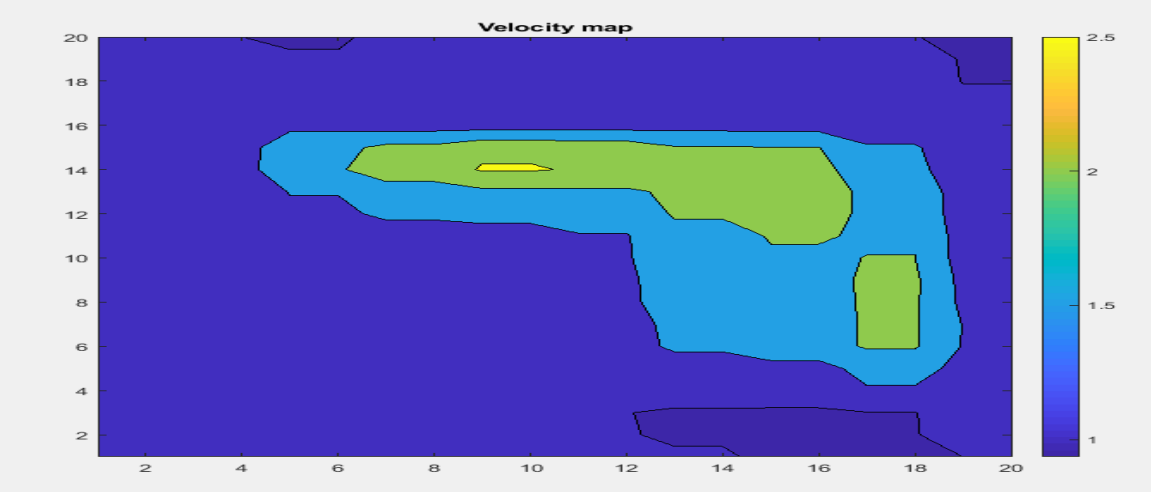

Fig (4.23): Synthetic model SIRT staggered inversion in regluar mesh; velocity map

The anomaly is shown clearly but with more reduced value of the velocity especially, from the random staggering fig (4.22, and increasing of high velocity areas, in the other hand the regular gives higher value to the anomaly in narrow area fig (4.23).

The residuals percentages show some enhancement from %10 in case of regular mesh staggering, and %9.7 with random mesh staggering.

4.6.2 Field data inversion results:

The results of sirt inversion carried out in real field data are as shown in table:(4.5), the statistics, spatial coverage plot, and ray density fig(4.26), and fig (4.27) regard the model before inversion. Fig (4.28), fig(4.29), fig(4.30) and fig (4.31) show the diagonal of the model resolution matrix and the data resolution matrix that reflect the assesment of the resoution of the sirt inversion algorithm.

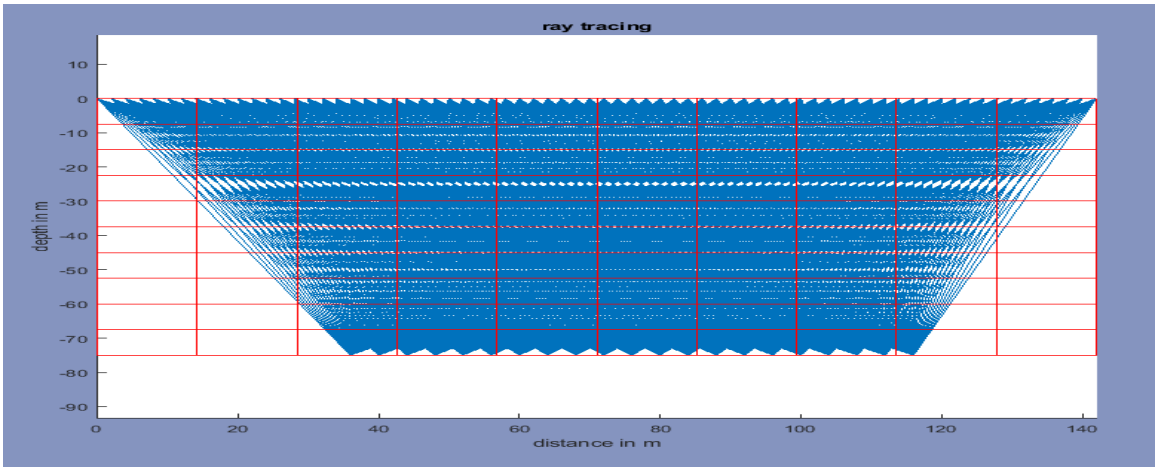

Fig (4.24): Field data SIRT inversion, coverage and raytracing

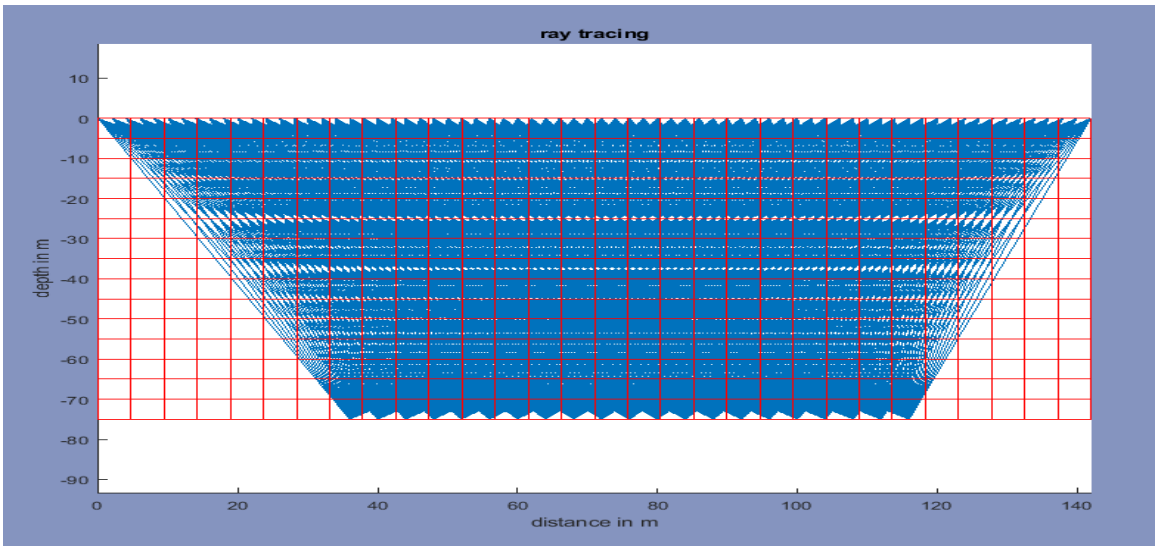

Fig (4.25): Field data SIRT inversion in fine grid, coverage and raytracing

➢ **Spatial coverage and Ray density:**

a) b)

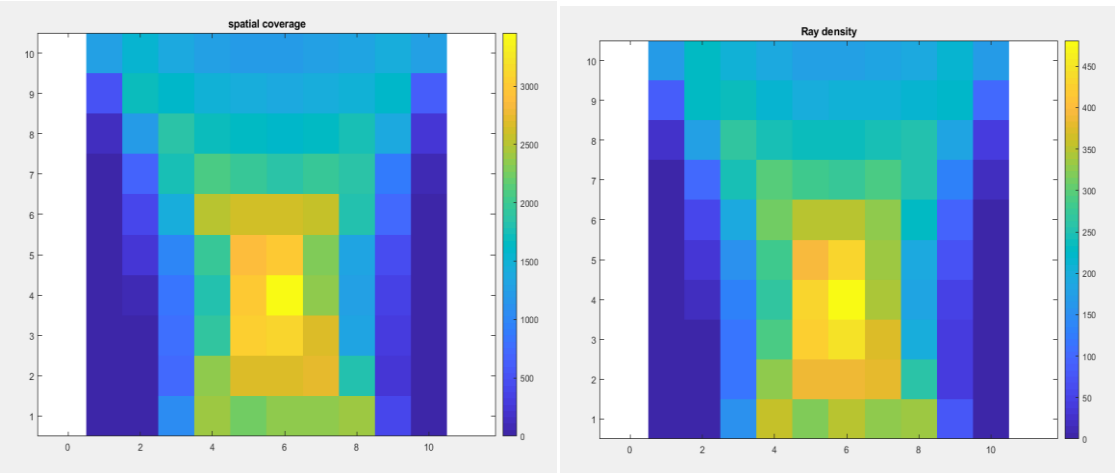

Fig (4.26): Field data SIRT inversion in coarse grid a) spatial coverage, b) ray density

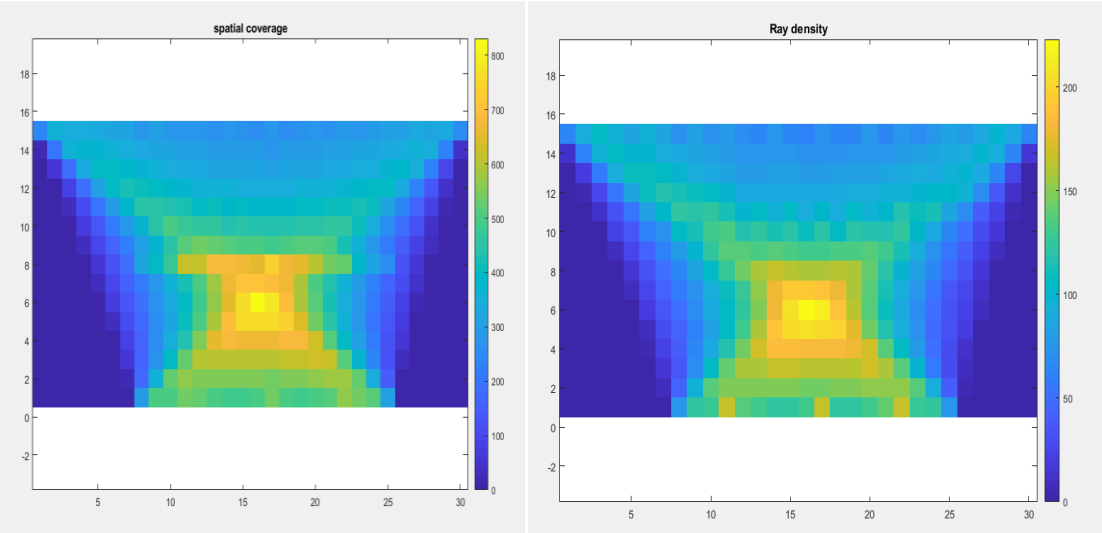

Fig (4.27): field data SIRT inversion in fine grid a) spatial coverage, b) ray density

- **Results of sirt inversion:**

Table (4.5): field data SIRTinversion results

parameter	Coarse (10*10)	Fine (30*15)
Rays eliminated (attraversing less cells)	21	21
Rays eliminated (high residuals)	68	68
Cells eliminated (less rays passed through the cell)	12	81
Factor of increment	1.2	1.2
No of iterations	29	31
Root mean square of residuals	%10.47	%10.24

The resolution matrix:

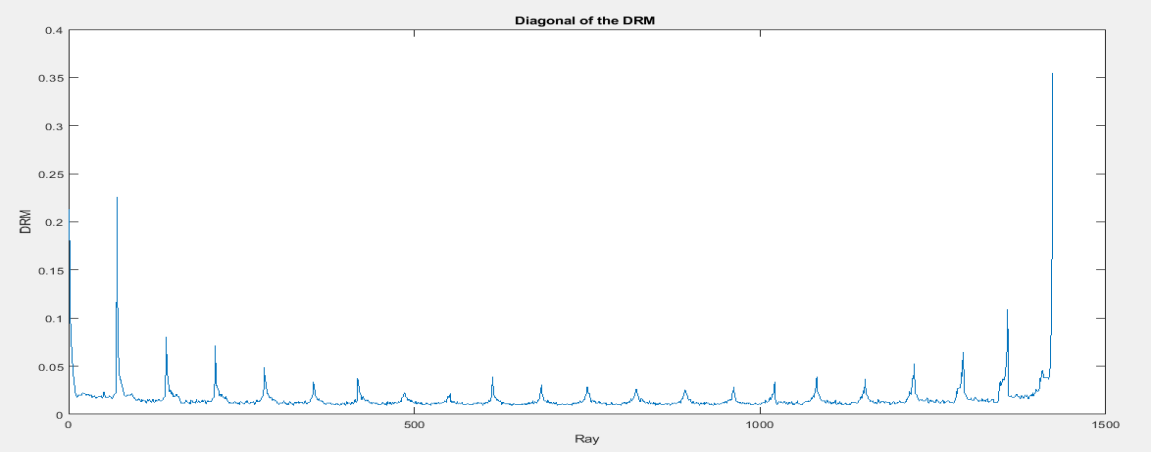

Fig (4.28): Field data SIRT inversion in coarse grid; Diagonal of DRM

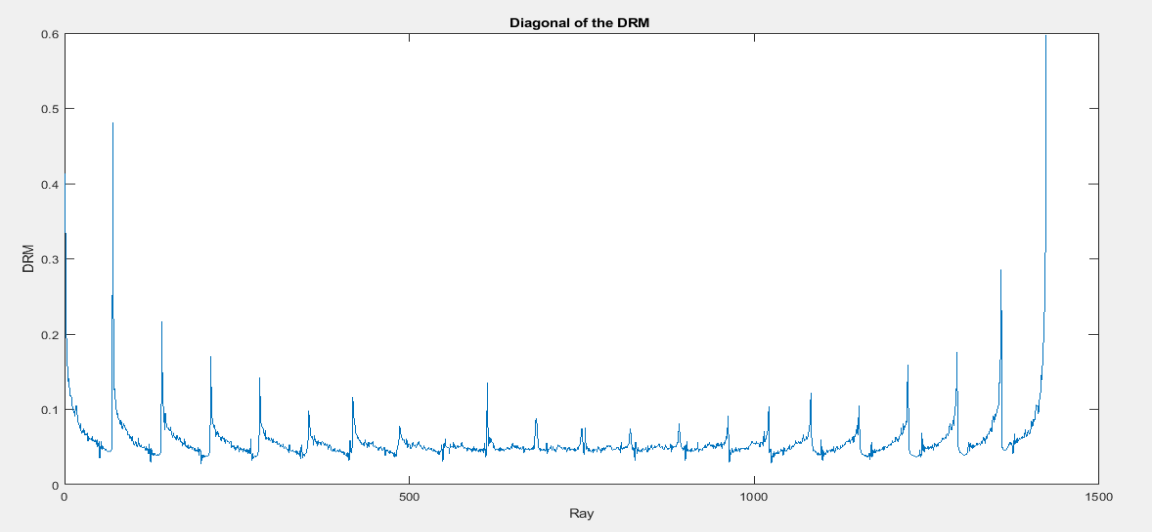

Fig (4.29): Field data SIRT inversion in fine grid; Diagonal of DRM

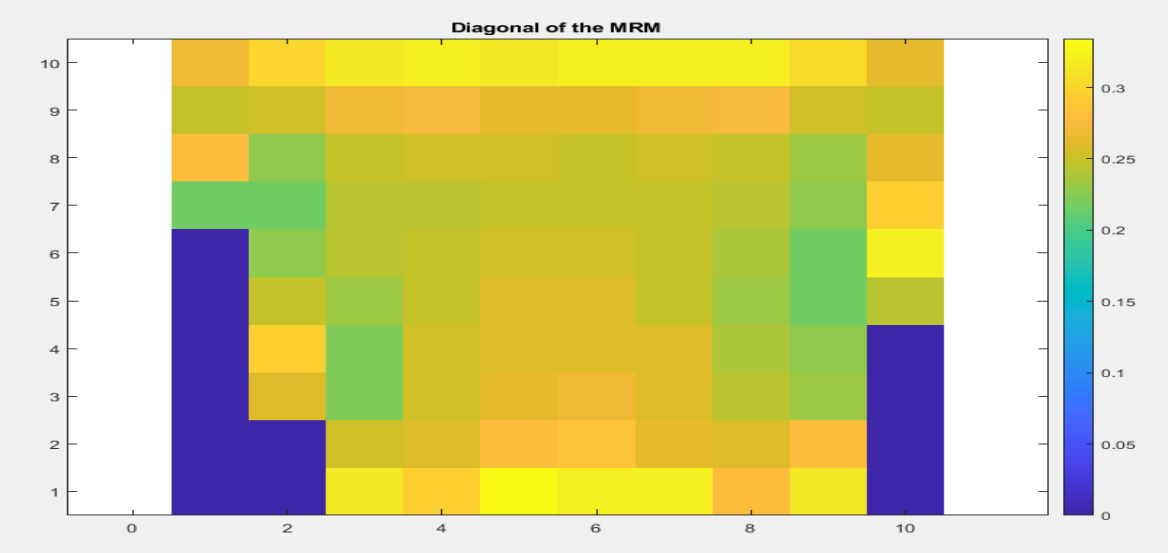

Fig (4.30):Field data SIRT inversion in coarse grid;Diagonal of MRM

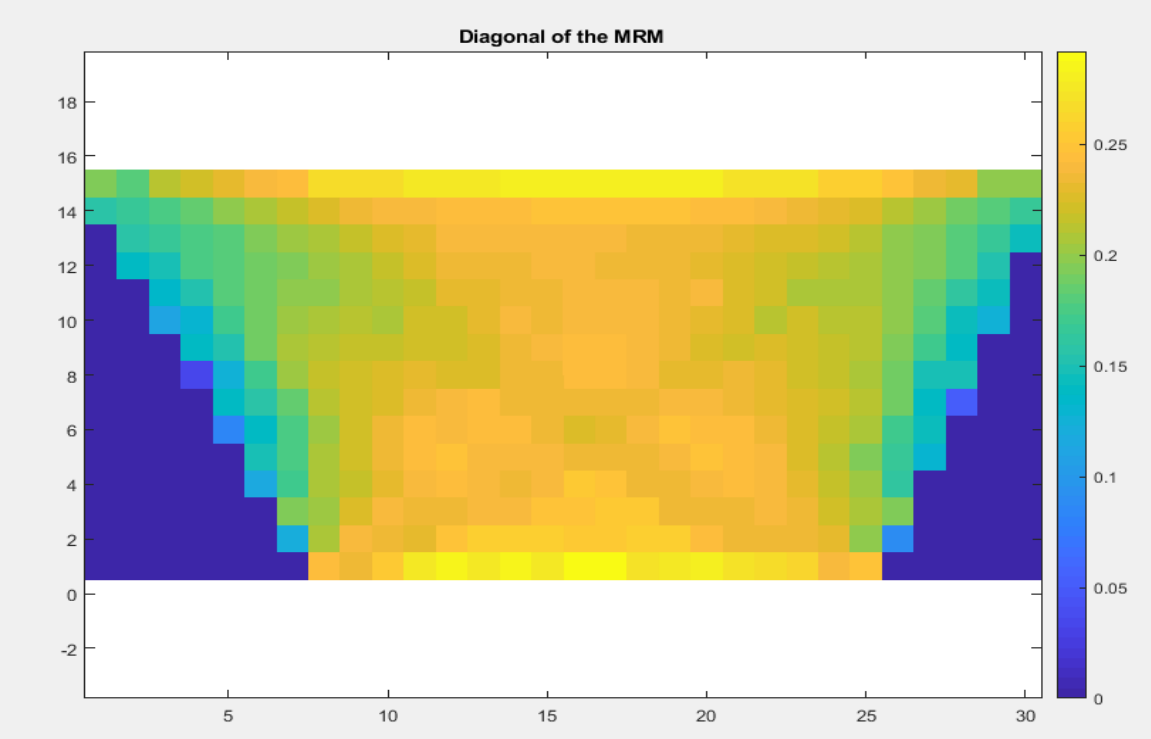

Fig (4.31): Field data SIRT inversion in fine grid; Diagonal of MRM

The data and model resolution matrices show almost same level of resolution according to the values of diagonal elements. Lower level of resolution observed in real data inversion compared to the synthetic model, this can be refered to picking errors, the same note can be said to residuals plots fig (4.32), fig(4.33), fig (4.34) and fig (4.35) which is a bit higher values than the synthetic residuls but show a gausian distribution more clear than the synthetic.

The velocity map fig (4.36), and fig (4.37) of both coarse and fine grids reflects same anomaly far right of the map but more detailed velocity distribution in case of fine grid. The values are almost equivalent.

➢ **Residuals:**

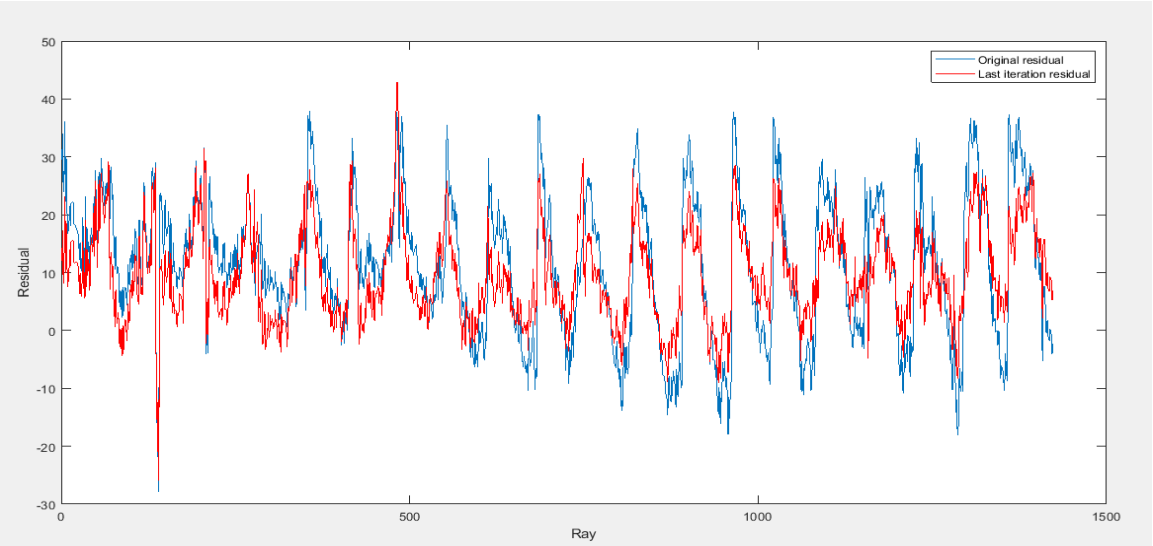

Fig (4.32): Field data SIRT in coarse inversion; plot of initial and final residuals

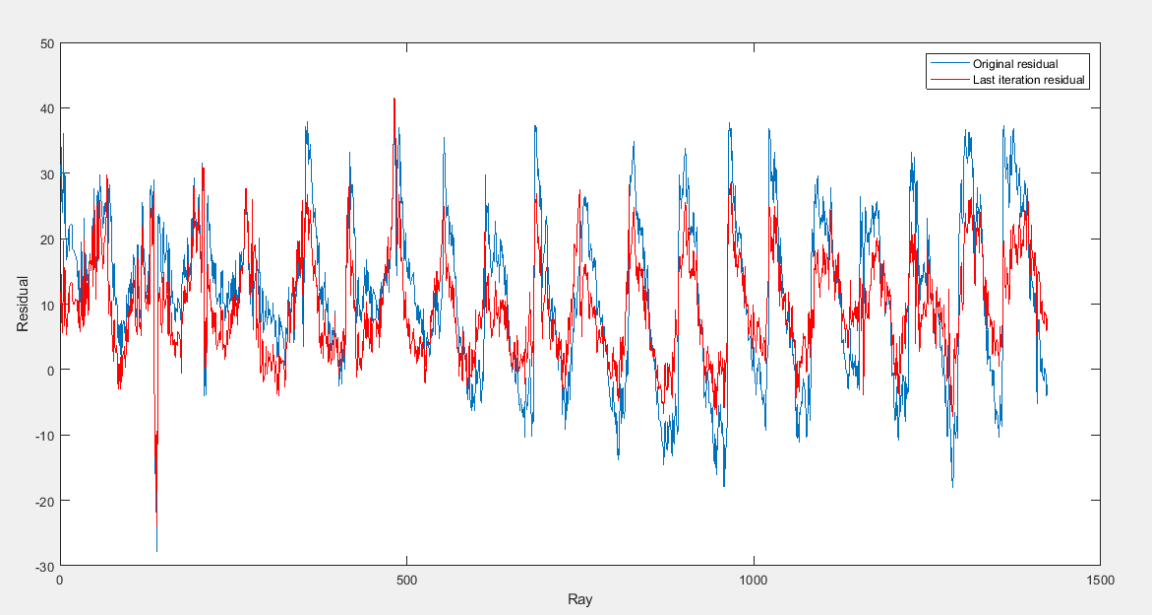

Fig (4.33): Field data SIRT inversion in fine grid; plot of initial and final residuals

a) b)

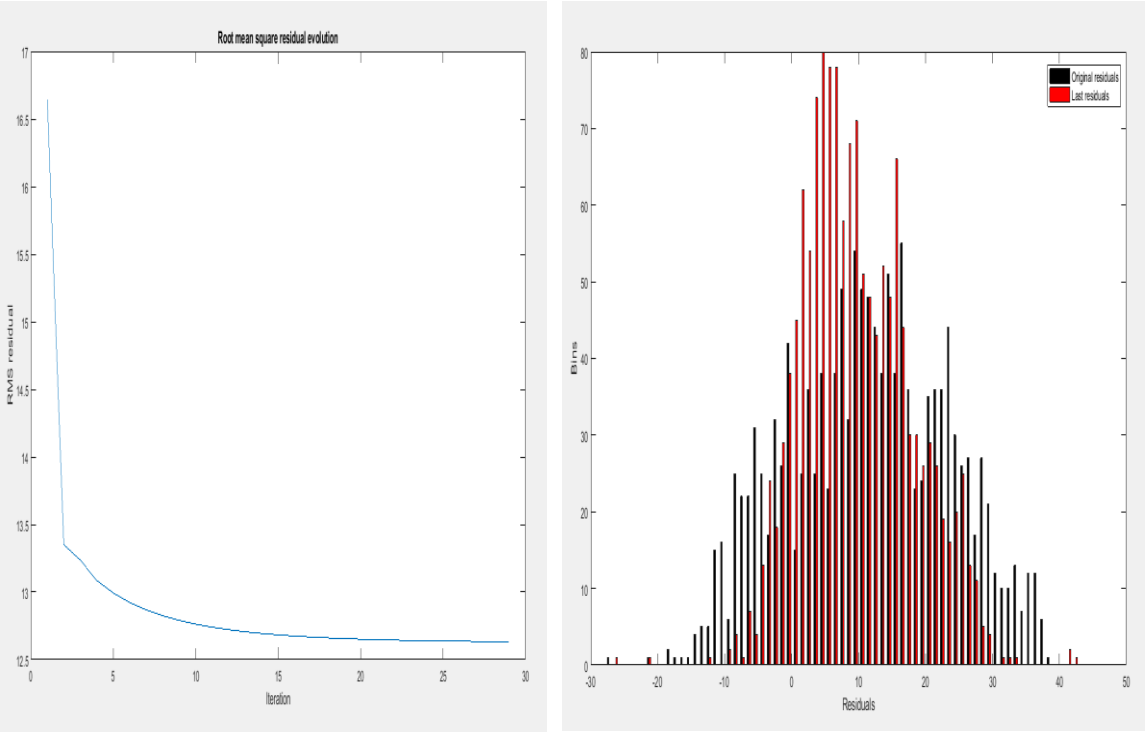

Fig (4.34): Field data SIRT inversion in coarse grid; a) residuals evolution, b) residuals histogram

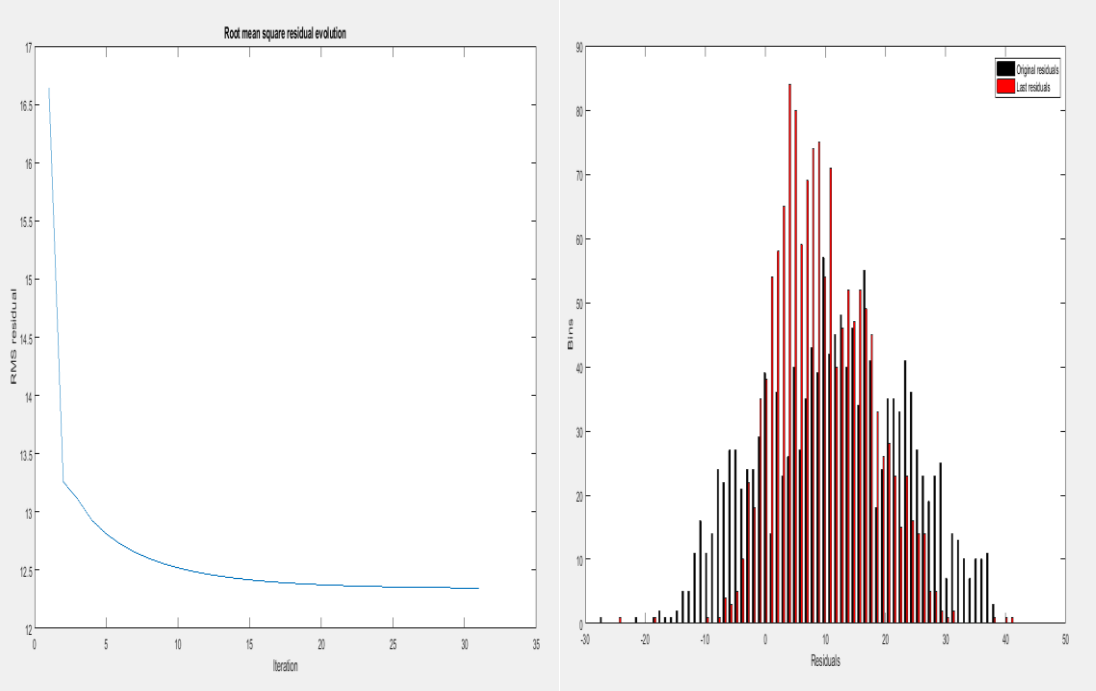

Fig (4.35): Field data SIRT inversion in fine grid; a) residuals evolution, b) residuals histogram

- **Velocity maps:**

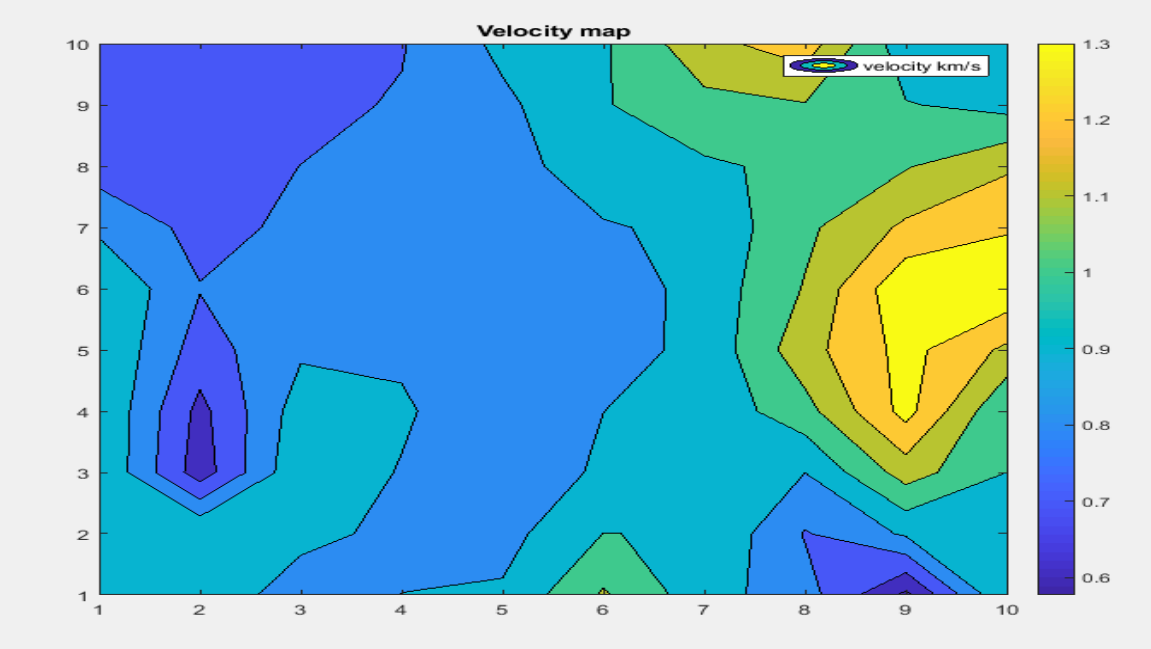

Fig (4.36): Field data SIRT inversion in coarse grid; velocity map

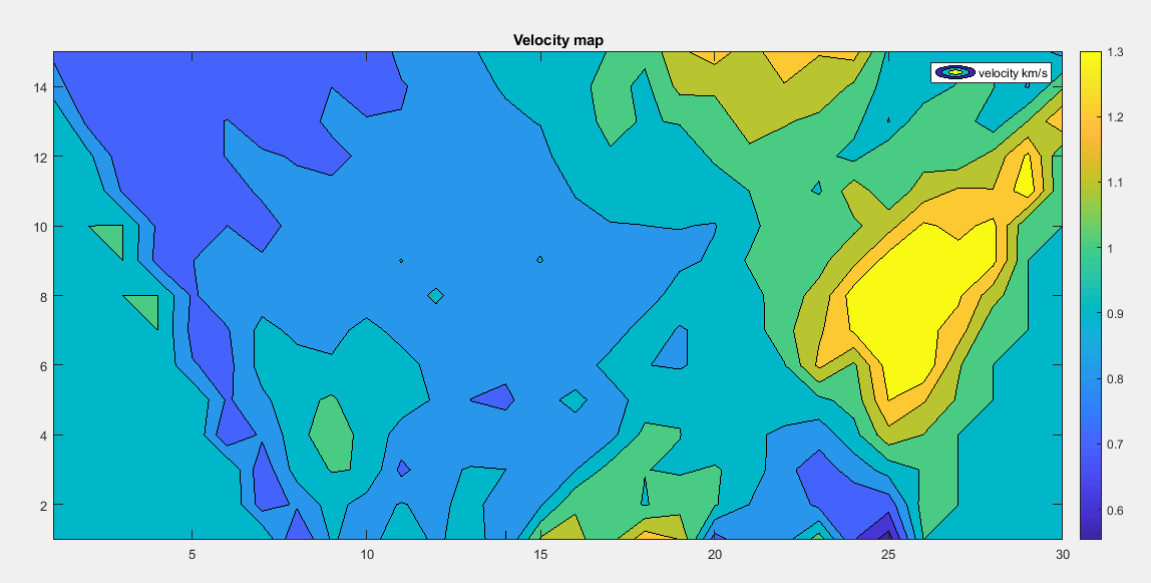

Fig (4.37): Field data SIRT inversion in fine grid; velocity map

- **Staggered inversion:**

Two inversion operations carried out; random mesh generated with a mesh generator, and another regular grid using 2 meshes for both and axes step equal to 2 units and it gave results shown in the table ().

Table (4.6): Field data SIRT staggered inversion results

parameter	1st mesh Random	2nd mesh random	1st mesh Regular	2nd mesh Regular
Rays eliminated (attraversing less cells)	21	21	21	21
Rays eliminated (high residuals)	68	68	68	68

Cells eliminated (less rays passed through the cell)	14	17	12	13
Factor of increment	1.2	1.2	1.2	1.2
No of iterations	27	27	29	28
Root mean square of residuals	%10.5842	%10.6096	%10.4693	%10.4716

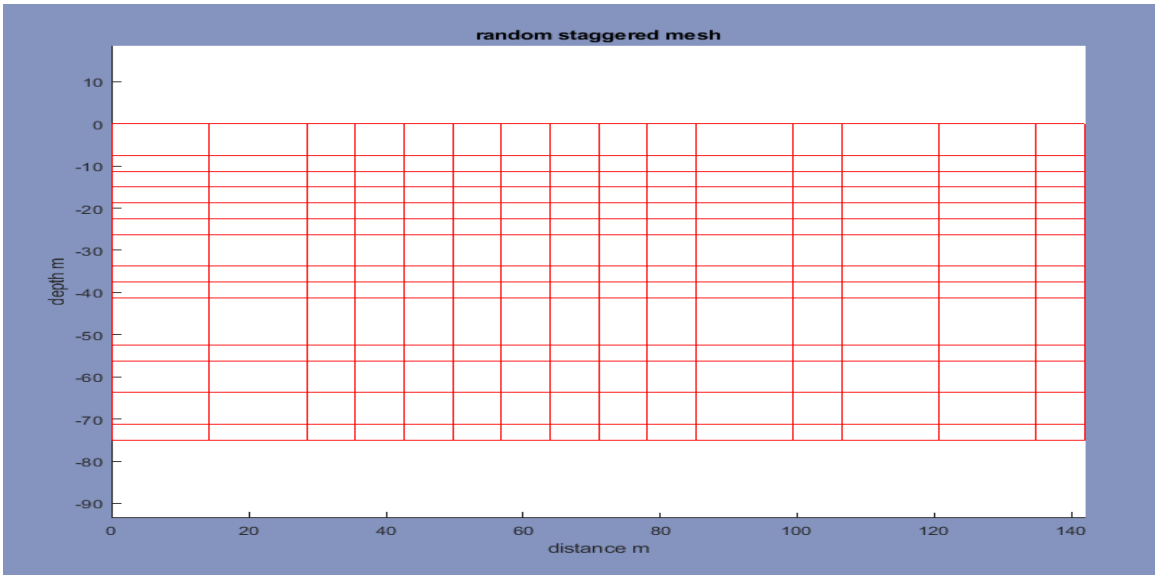

Fig (4.38): Field data SIRT inversion in staggered grid; irregular mesh

And yield the random staggered velocity map as average of 2 meshes shifting velocity values resampled and reconstructed Fig (4.37).

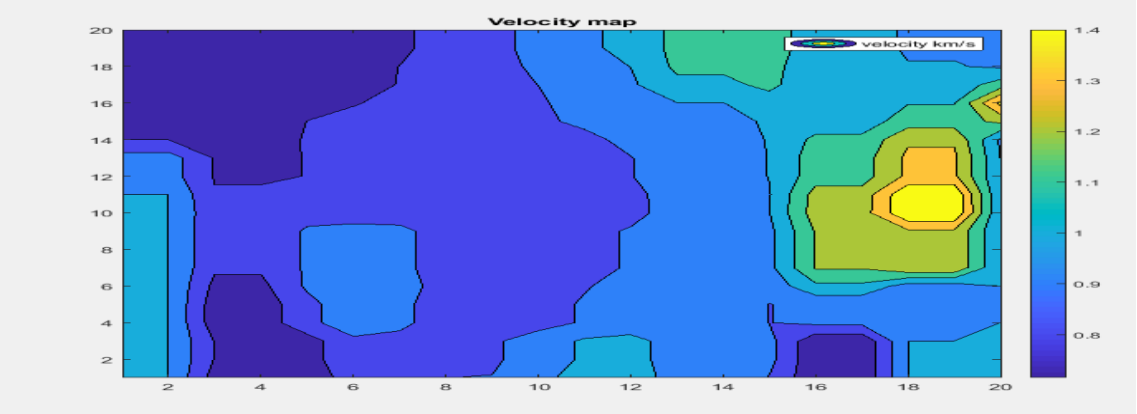

Fig (4.39): Field data SIRT staggered inversion in irregular grid; velocity map

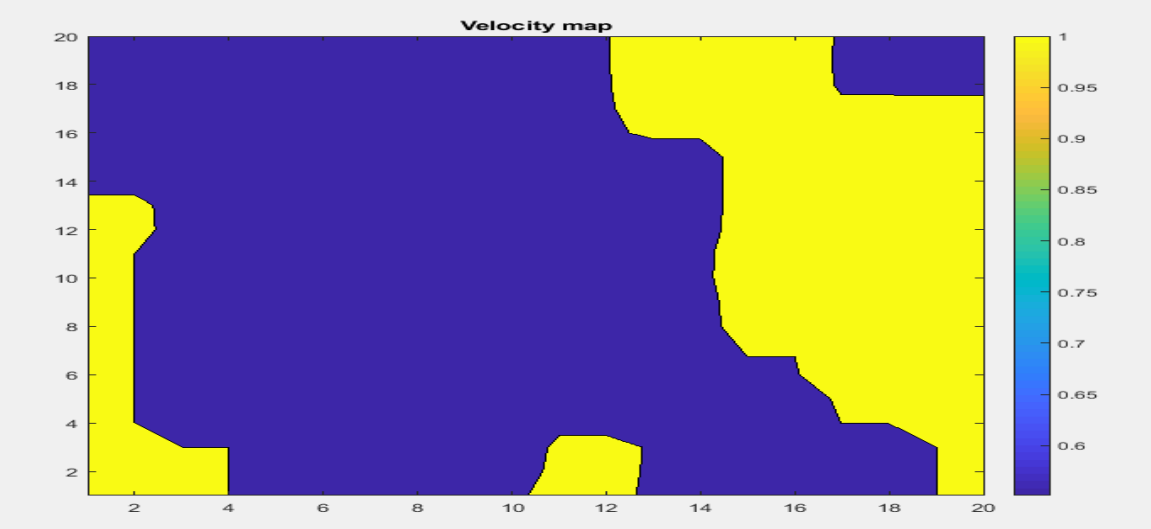

Fig (4.40): Field data SIRT staggered grid inversion in regular mesh

The most important output are the velocity map and the misfit root mean square value after several iterations. We got a misfit (traveltime residual) value of 12 ms in both grids. The velocity map reflects the anomaly in smooth way for random mesh staggering fig (4.39), but failed to image velocity distribution properly in regular mesh staggering.

Chapter five: Conclusions and Recommendations

5.Chapter five: Conclusions and Recommendations

5.1. Conclusions:

The objectives of the thisis are to apply the staggered grid inversion and test its resolution enhancement. The software used is Staggered Grid Random Tomography SGRAT invented by Prof. Godio and Prof. Sambuelli. The software was built to use Simultaneous Iterative Reconustruction Technique SIRT and Conjugated Gradient algorithms as basic inversion algorithms; then staggering take place by averraging the solutions and resampling the model.

Some minor errors have been recovered and new plots have been added to the software. The test carried out using only SIRT inversion algorithm on synthetic model and field data. The results show good results in SIRT inversion of both cases of inversion using either coarse grid or fine grid. Fast convergence observed especially in coarse grid due to the cells number utilized.Velocity maps generated by the software generally reflects the anomaly and its value with acceptable accuracy for some extent.Use of fine grid increases value of diagonal resolution matrix for both data, and model parameter. The effect of fine grid appears in more detailed anomaly distribution and less error percentage in the range of over-determined inverse problem.

Staggered grid gives reliable results equivalent to the fine grid inversion, especially when associated with a random basic grid. The SIRT inversion relibility reduced when it comes to the field data due to the level of uncertainity of the data (picking errors) and lacking of piriori information. Regarding velocity map, the anomaly appeared clearly and smoothed in case of irregular (random) mesh inversion, but it was biased in regular grid inversion.

For further studies, it is recommended to test the staggered grid on Conjugated gradient algorithm and to introduce parallel computing to reduce time of computation.

Reference and Bibliography

Reference and Bibliography

A. Arato, A. Godio, and L. Sambuelli. (2014). staggered grid inversion of cross hole 2-D resistivity tomography. *Journal of applied geophysics* , 60-70.

A. L. Imhof, C. A. Calvo, and J. C. Santamarina. (2010). SEISMIC DATA INVERSION BY CROSS-HOLE TOMOGRAPHY. *Brazilian Journal of Geophysics* , 79-88.

Alessandro., A. (2013). *2-D and 3-D tools for electrical imaging in environmental applications.* turin: Politecnico di Torino.

Berryman, J. G. (1991). *Lecture notes on non linear inversion and tomography.* Livermore, California.

C. Thurber, and J. Ritsema. (2007). *Theory and Observations – Seismic Tomography.* Elsevier B.V.

F. I. Louis, K. C. Makropoulos. (2005). Image enhancement in seismic tomography by grid handling: Synthetic simulations with fault-like structures. *JOURNAL OF BALKAN GEOPHYSICAL SOCIETY* , 10.

Gruber, T. (1998). *Crosshole seismic tomography incorporating later arrivals, Phd thesis.* University of Adelaide, Australia.

J.M.Lees, and R.S. Crosson. (1991). Bayesian ART versus conjugate gradient methods in tomographic seismic imaging: An application at Mount St. Helens. *Spatial Statistics and Imaging,* , 186-208.

L Sambuelli, G Bohm, P Capizzi, E Cardarelli and P Cosentino. (2011). Comparison between GPR measurements and ultrasonic tomography with different inversion algorithms: an application to the base of ancient Egyptian sculpture. *Journal of Geophysics and Engineering* , 12.

Lees, J.M., and R.S. Crosson,. (1991). Bayesian ART versus conjugate gradient methods in tomographic seismic imaging: An application at Mount St. Helens. *Spatial Statistics and Imaging,* , 186-208.

M. Aravinitis, B.D. Al-Nazi. (2009). Mathematical representation models and applications on seismic tomography. *NAFTA* , 495-498.

N. Rawlinson, and W. Spakman. (2016). On the use of sensitivity tests in seismic tomography. *Geophysical Journal International* , 1221-1243.

Nolet, G. (2008). *A one day course of Seismic tomography.* Trieste: The Abdus Salam International Center for Theoretical Physics.

R. L. Nowack, and C. Li. (2009). seismic tomography. In a. C. R. L. Nowack, *Handbook of Signal Processing in Acoustics* (pp. 1635-1653). Springer-VerlagEditors: D. Havelock, S. Kuwano, M. Vorlander.

Rawlinson, N. (1996). *Methods and Codes used in Seismic Tomography.* Canberra, Australia: Australian Geological survey organization.

S. K. Nath, S. Chakraborty, S. K. Singh, and N. Ganguly. (1999). Velocity inversion in cross-hole seismic tomography bycounter-propagation neural network, genetic algorithm and evolutionary programming techniques. *Geophysics Journal International* , 108-124.

Scales, J. (1987). Tomographic inversion via the conjugate gradient method. *Geophysics* , 179-185.

Schleicher, K. (2018). The conjugate gradient method. *The leading Eadge* , 296-298.

Tape, C. (2009). *seismic tomography of southern California using adjoint methods.* Pasadena, California: California Inistitute of Technology.

W. Cao, S. M. Hanafy, G. T. Schuster, G. Zhan and C. Boonyasiriwat. (2012). High-resolution and super stacking of time-reversal mirrors in locating seismic sources. *Geophysical prospecting* , 1-17.

W. Huang, H. Zhou. (2015). Least Squares Seismic Inversion with Stochastic Conjugate Gradient Method. *Journal of Earth Science* , 463-470.

Y. Rao, Y. Wang, S. Chen, and J. Wang. (2016). Crosshole seismic tomography with cross-firing geometry. *Geophysics Vol 81, NO. 4* , Society of Exploration Geophysicest.

Zhao, D. (2015). *Multi scale seismic tomography.* Sendai, Japan: springer geophysics.